

## Chapter 4

# Electrochemically Programmed, Spatially Selective Functionalization of Silicon Nanowires

### 4.1 Introduction

The spatially selective biofunctionalization of surfaces has proven to be an enabling capability, beginning with the early work of Fodor and co-workers<sup>1</sup> on utilizing photolabile surface groups to construct DNA libraries, to the use of inkjet technologies for the construction of protein chips.<sup>2</sup> The dip-pen lithography methods from Mirkin's group represent the current limit of patterning density for protein chips.<sup>3</sup> Chip-based array methods are largely predicated upon the optical detection of the target/probe binding events, which imposes the optical diffraction limit on pixel density. However, electronically transduced detectors, such as chemically gated silicon nanowires (SiNW),<sup>4,5</sup> may circumvent this limitation. Methods for fabricating ultra-high density circuits of silicon nanowires<sup>6</sup> with excellent conductivity<sup>7</sup> and field-effect transistor<sup>8,9</sup> properties required for biosensors have been established. To construct an array of sensors, NWs must be functionalized with different receptor probes, such as antibodies or aptamers, against their designated molecular targets. Here we describe an electrochemical approach that, while possibly having multiple applications, should be applicable toward the selective biopassivation of silicon nanowire sensor arrays, and is spatially limited only by the ability to electronically address the individual sensor elements.<sup>10</sup>

Recent advances in alkylation of H-terminated Si surfaces has made it possible to bypass the necessity of chemical modification of the native oxide of silicon.<sup>11-13</sup> Hydrosilylation produces cleaner, more stable and more reproducible monolayers than silane-based SAMs.<sup>14</sup> The benefits of utilizing organic monolayers formed on H-terminated Si for biosensing are multifold. First, the removal of the SiO<sub>x</sub> tunneling barrier brings the target/probe pair 1-2 nm closer to the conducting surface,<sup>15</sup> which, as we have previously reported,<sup>5</sup> translates into an increase in the sensitivity of the device. Second, the electrical properties of sufficiently small diameter silicon NWs are dominated by the surface characteristics. Removal of what is often an electrically imperfect Si-SiO<sub>2</sub> interface and a disordered oxide film with a high density of trap sites<sup>16</sup> is desirable. Finally, the difficulty in controlling the smoothness of the SiO<sub>2</sub> layer results in rough and grainy surfaces upon the growth of the siloxane-anchored monolayers.<sup>17, 18</sup>

Alkyl monolayers grown on appropriately prepared H-terminated Si(111) can reflect the atomic flatness of the underlying substrate.<sup>19, 20</sup> Multiple studies have focused on the methods of chemical passivation of silicon via a formation of Si-C bond. Hydrosilylation has been accomplished with radical initiators,<sup>21, 22</sup> through thermally induced<sup>14, 22-26</sup> or photochemical methods,<sup>27-31</sup> or utilizing Lewis acid catalysts.<sup>32, 33</sup> Alkylmagnesium reagents have been successfully employed for the alkylation of H-terminated Si surfaces,<sup>34, 35</sup> and halogenated surfaces have been alkylated with alkylmagnesium and alkyllithium reagents.<sup>28, 36-40</sup> Furthermore, electrochemical methods of H-terminated silicon functionalization have been explored.<sup>41</sup> Several research groups have demonstrated an ability to utilize these functionalization methods to nonspecifically attach DNA to silicon surfaces.<sup>42-44</sup>

Electroactive monolayers have attracted attention due to the growing interest in selective molecular and cellular immobilization on surfaces. Electrochemical activation of hydroquinone<sup>45, 46</sup> and hydroquinone esters on gold,<sup>47</sup> as well as oxidation of thiols on Si-SiO<sub>2</sub> surfaces<sup>48</sup> have been demonstrated for such applications. Notably, Mrksich's group has accomplished a selective attachment of proteins and cells to monolayers on gold via a Diels-Alder reaction between 1,4-benzoquinone and cyclopentadiene.<sup>45, 46</sup> Here, we extend this chemistry of hydroquinone terminated monolayers<sup>49</sup> to H-terminated silicon surfaces. We also demonstrate an alternative method of molecular attachment via Michael addition of thiol-terminated molecules to *p*-benzoquinone.<sup>50, 51</sup> In addition, we discuss strategies to reduce biofouling by utilizing mixed monolayers consisting of electroactive molecules and oligo(ethylene glycol).<sup>52, 53</sup> Finally, we discuss an alternative electrochemical functionalization strategy which utilizes reductively driven electroactive molecule that has been "clicked" to the acetylenylated silicon surface.<sup>54</sup> Such strategy avoids deleterious oxidative damage of the silicon surface, which is detrimental to solution sensing applications.

## 4.2 Experimental Methods

### 4.2.1 Materials

Single-polished Si(111): n-type, 550  $\mu\text{m}$  thick, resistivity 0.005-0.02  $\Omega\cdot\text{cm}$  (Montco Silicon Technologies), single-polished Si(100): n-type, 500  $\mu\text{m}$  thick, 0.005-0.01  $\Omega\cdot\text{cm}$  (Wacker-Chemitronic, Germany), and silicon-on-insulator (SOI) (100): n-type, 9-18  $\Omega\cdot\text{cm}$ , 50 nm device thickness, 145 nm buried oxide thickness (Ibis Technology Corp.), substrates were used. All reagents used were of highest purity. Streptavidin-AlexaFluor and



**Molecule A.** 2-(4-(tetrahydro-2H-pyran-2-yloxy)phenoxy)-tetrahydro-2H-pyran was synthesized according to literature methods.<sup>55</sup> To a solution of THP protected hydroquinone (4.26 g, 15 mmol) in THF, was added t-butyllithium (15 mL of 1.7M solution in pentane) dropwise at -78 °C. The reaction mixture was stirred at room temperature for 2 hours, followed by the addition of 12 mL of 11-bromo-1-undecene, and then stirred overnight at 40 °C. The reaction mixture was diluted with ethyl acetate, washed with saturated NH<sub>4</sub>Cl and brine, then dried over MgSO<sub>4</sub>. Column chromatography with 1:1 hexane/dichloromethane gave mg (60% yield) of molecule A as a colorless oil. <sup>1</sup>H NMR (CDCl<sub>3</sub>, 300MHz) δ 6.99 (m, 1H), 6.84 (m, 2H), 5.81 (m, 1H), 5.29 (s, 2H), 4.95 (m, 2H), 3.91 (m, 2H), 3.59 (m, 2H), 2.58 (t, 2H), 1.62-2.02 (m, 28H)

**Molecule B.** 11-(2,5-dimethoxyphenyl)-1-undecene was synthesized by following the procedure outlined in the literature.<sup>56</sup> To a solution of 2.76 g (0.02 moles) of p-dimethoxybenzene in 20 mL THF was added dry tetramethylethylenediamine (2.19 mL, 14.5 mmol). The solution was cooled to -78 °C and purged under argon. N-butyllithium in hexanes (1.6M, 12.5 mL) was slowly added and the resulting pale yellow reaction was stirred for 2 hours. Subsequently, solution of 11-bromo-1-undecene (4.3 mL, 19.6 mmol) was added. The colorless reaction mixture was stirred for 12 hours after it was warmed up to room temperature. The mixture was diluted with ethyl acetate, washed with saturated NH<sub>4</sub>Cl solution, water and brine and dried over MgSO<sub>4</sub>. The concentrated pale yellow organic oil was purified by column chromatography with hexane/dichloromethane (500 mL 1:10, 500 mL 1:5, 500 mL 1:3) to afford 3.2g (55% yield) of product as colorless oil: <sup>1</sup>H NMR (CDCl<sub>3</sub>) δ 6.74 (m, 3H, -C<sub>6</sub>H<sub>3</sub>(OCH<sub>3</sub>)<sub>2</sub>), 5.82 (m, 1H, -CHCH<sub>2</sub>), 4.96 (dq, J = 2.0 and

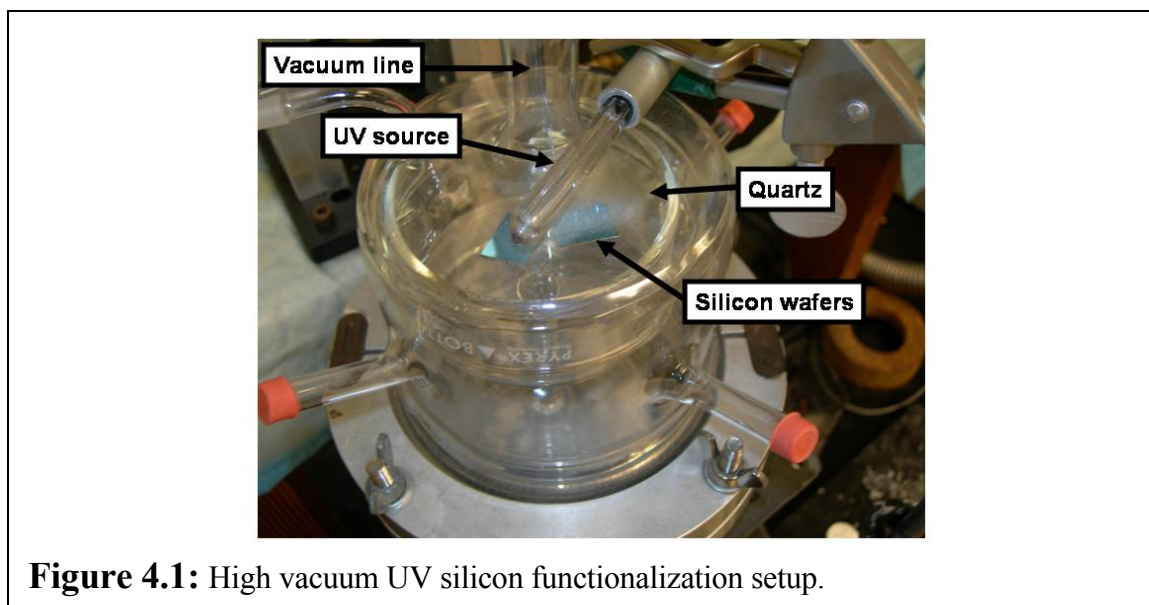
17.1 Hz, 2H, -CHCH<sub>2</sub>), 3.78 (s, 3H, -OCH<sub>3</sub>), 3.77 (s, 3H, -OCH<sub>3</sub>), 2.57 (t, J = 7.6 Hz, 2H, -CH<sub>2</sub>-Ar), 2.03 (q, J = 6.7 Hz, 2H, -CH<sub>2</sub>CHCH<sub>2</sub>) 1.57 (br s, 2H, -CH<sub>2</sub>CH<sub>2</sub>-Ar) 1.29 (br s, 12H, -(CH<sub>2</sub>)-).

**Molecule E.** Previously reported method<sup>57</sup> was modified to synthesize molecule E as follows. To a solution of 50 mL triethylene glycol (375 mmol) in dry dimethylformamide (DMF) was added 3.06 g NaH (60% in mineral oil, 76.5 mmol). After four hours, 12 mL 11-bromo-1-undecene (54.7 mmol) was added and the reaction was left overnight. DMF was evaporated and the resulting oil was diluted in DCM. After several extraction steps with DCM, the solution was dried over Na<sub>2</sub>SO<sub>4</sub> and concentrated. The product was purified by column chromatography with ethyl acetate/hexanes (1:3) to afford 14.67 g of clear oil (88.7% yield): <sup>1</sup>H NMR (CDCl<sub>3</sub>) δ5.7 (m, 1H, -CHCH<sub>2</sub>), 4.9 (m, 2H, CHCH<sub>2</sub>), 3.5-3.7 (d, 12H, -OCH<sub>2</sub>CH<sub>2</sub>OCH<sub>2</sub>CH<sub>2</sub>OCH<sub>2</sub>CH<sub>2</sub>OH), 3.42 (t, 2H, J=7Hz, CH<sub>2</sub>CH<sub>2</sub>CH<sub>2</sub>O-), 2.8 (br s, 1H, -OH), 2.0 (q, 2H, J=7Hz, -CHCH<sub>2</sub>-), 1.55 (qui, 2H, J=7Hz, -CH<sub>2</sub>CH<sub>2</sub>CH<sub>2</sub>O-), 1.25 (br s, 12H, -CH<sub>2</sub>CH<sub>2</sub>-). To 3 g of the above purified undec-1-en-11-yltri(ethylene glycol) in dry DMF was added 0.23 g NaH (2 mmol) and allowed to react for 2 hours at room temperature. Subsequently, 2.84 g of iodomethane (20 mmol) was added and the reaction was left overnight at 40 °C to produce pale yellow solution. The concentrated clear oil was purified on silica gel with DCM/hexanes (1:1) to afford 0.92 g of clear oil (30% yield).

### 4.2.3 Surface Functionalization

Si(111) and Si(100) substrates were cleaned in piranha (H<sub>2</sub>SO<sub>4</sub>:H<sub>2</sub>O<sub>2</sub> = 2:1) at 90 °C for 15 minutes and etched in degassed 40% NH<sub>4</sub>F [Si(111)] for 20 minutes or in 2.5%

HF for 15 seconds, respectively. In the case of SOI substrates, wafers were spin-on doped with phosphorosilica film to concentrations of  $10^{18} \text{ cm}^{-3}$  as measured with 4-point probe (chapter 2). The top 50 nm Si layer was patterned using conventional photolithography on AZ5214 photoresist and etched in  $\text{SF}_6$  by reactive ion etching (RIE). In the case of nanowires, scanning electron microscopy (SEM) was utilized to pattern the PMMA e-beam



resist. After acetone liftoff, the substrate was cleaned in ALEG (J.T. Baker Microelectronics) at  $90^\circ\text{C}$  for 15 minutes and etched with 2.5% HF for 2 seconds. Immediately after etching, neat degassed (by freeze, pump, thaw cycles) Molecules A or B (Scheme 4.1) were spotted onto the chip. The samples were immediately placed into custom-made quartz chamber, which was then attached to the vacuum line and pumped down (Figure 4.1). Functionalization was carried out for 2 hours with UV (254 nm,  $9 \text{ mW/cm}^2$ ) illumination under  $\sim 10^{-5}$  Torr. Chips were rinsed with  $\text{CH}_2\text{Cl}_2$ , deprotected with either 1% TSA in methanol (Molecule A) or with  $\text{BBr}_3$  in anhydrous DCM (Molecule B). After deprotection, a  $15^\circ$  to  $20^\circ$  drop in contact angle was observed.

To selectively attach molecules to the silicon wires, functionalized device was fixed into a custom-made Teflon cell so that only the center of the chip was in contact with solution. Individual wires were then connected to the outside metal pins with a thin gold wire using silicon-indium-gold contacts. Wires were oxidized at 700mV (vs. Ag/AgCl) for 5 seconds. Immediately after the oxidation the devices were left in the solution of 10mM Molecule C (1:1 DPBS:MeOH) for 30 minutes. Subsequently, the chips were sonicated in methanol for 10 minutes and streptavidin-AlexaFluor (10nM in DPBS) or streptavidin-Au (10pM with 0.05% Tween20 in DPBS) conjugate was introduced for 5 to 10 minutes. Devices were sonicated in 0.05% Tween20/DPBS for 20 to 30 minutes. In the case of Nanogold streptavidin detection, the nano-particles were amplified with silver enhancement reagents for 20 minutes.

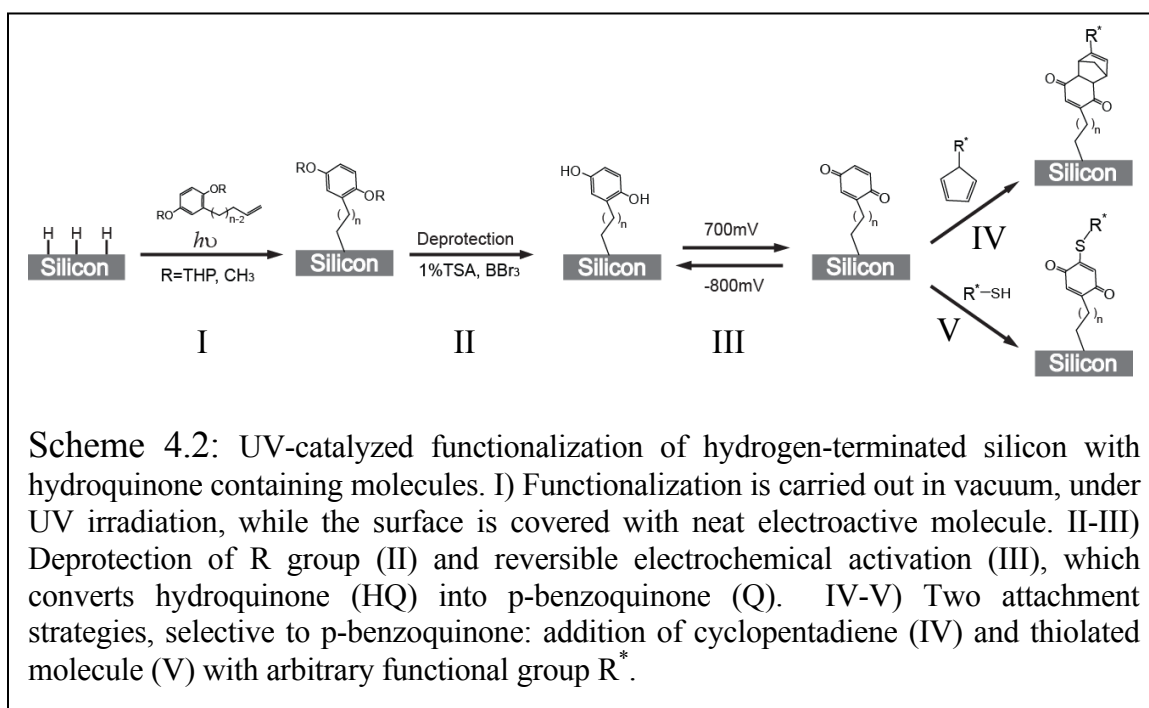
#### **4.2.4 Electrochemistry, XPS, and Optical Microscopy**

Electrochemistry of monolayers on bare silicon was performed in custom made cells with VersaStat II (EG&G Instruments). DPBS (see materials section) was used as the electrolyte, with Pt counter and Ag/AgCl (BAS Instruments) reference electrodes. For the determination of molecular coverage, the area under the cathodic peak was converted to the number of molecules through a stoichiometric ratio of 2 electrons to 1 electroactive molecule, divided by electrode surface area and normalized to Si atom surface density ( $7.8 \times 10^{14}$  for Si(111) and  $6.8 \times 10^{14}$  for Si(100)). XPS was performed in a UHV chamber that has been described elsewhere.<sup>58</sup> Experiments were performed at room temperature, with 1486.6 eV X-ray from the Al K $\alpha$  line and a 35° incident angle measured from the sample surface. ESCA-2000 software was used to collect the data. An approach described elsewhere<sup>58, 59</sup> was used to fit the Si 2p peaks and quantify the amount of surface SiO<sub>x</sub>,

assuming that the oxide layer was very thin. Any peak between 100 eV and 104 eV was assigned to  $\text{Si}^+-\text{Si}^{4+}$  and fitted as described in the literature.<sup>60</sup>  $\text{SiO}_x:\text{Si}$  2p peak ratio was divided by a normalization constant of 0.21 in the case of Si(111) and 0.17 in the case of Si(100).<sup>59</sup> Fluorescence spectroscopy was performed on Nikon Eclipse  $\epsilon 800$  microscope with a D-eclipse C1 confocal system equipped with 488nm, 546nm and 633nm sources.

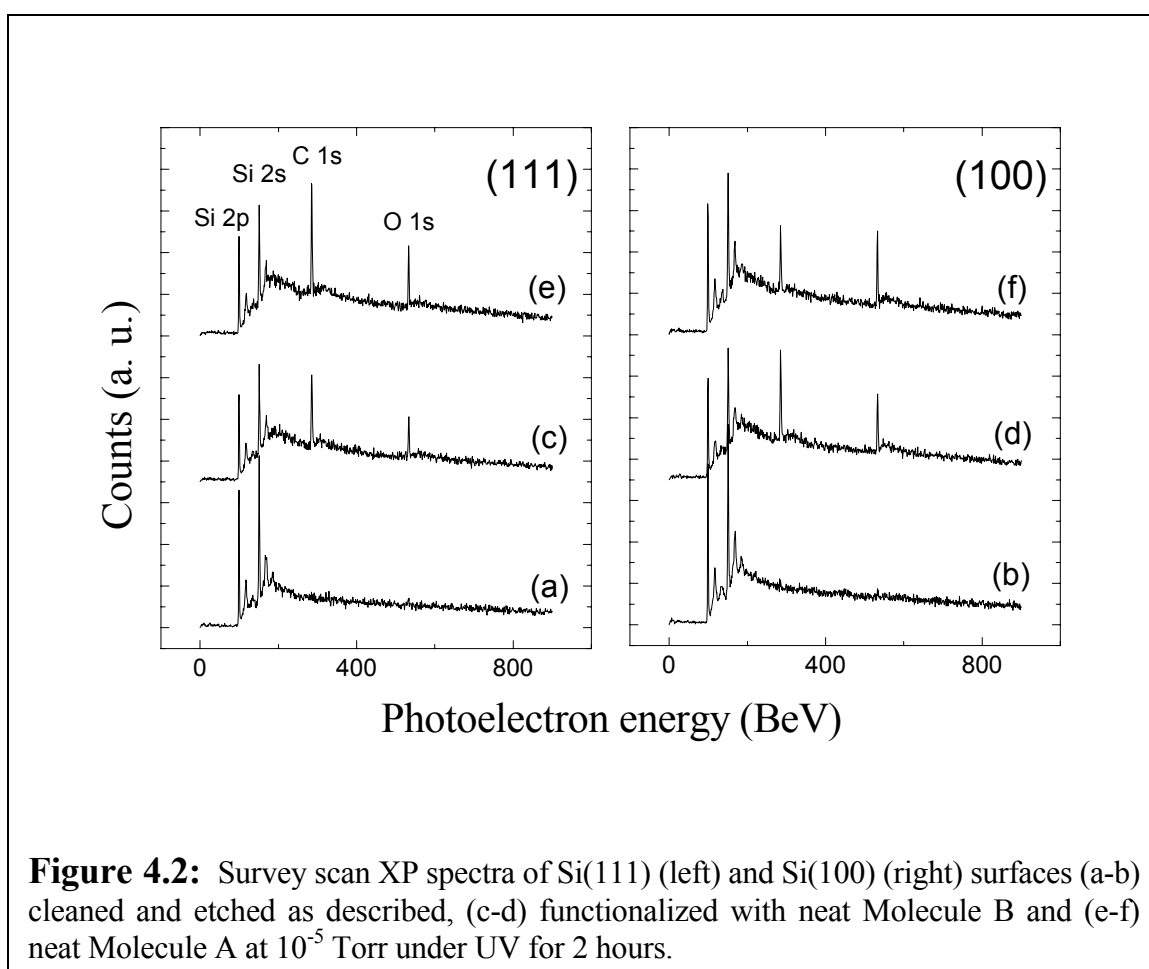
### 4.3 Functionalization of Hydrogen-Terminated Si(111) and Si(100) Surfaces with Hydroquinone

#### 4.3.1 Characterization of Electroactive Organic Monolayers



Scheme 4.2 shows the overall strategy of spatially-selective immobilization via a Diels-Alder reaction (Step IV) or Michael addition (Step V). The initial step in organic monolayer formation on H-terminated silicon involves a wet etch of native oxide. We employed an established wet etch (40%  $\text{NH}_4\text{F}$ ) for preparing atomically flat Si(111).<sup>61</sup>

However, the flattest Si(100) surface that can be generated by a wet etch is substantially rougher, with (111) facets, and is thus more prone to oxidation.<sup>62-64</sup> Our SNAP method for NW fabrication can be carried out most easily using silicon-on-insulator (SOI) substrates,<sup>6</sup> which are commercially available mostly in the (100) orientation. Bonded Si(111) wafers are also available, although they require substantial additional processing steps before being suitable for NW fabrication. Thus, the Si(111) surface is more ideal, while the Si(100) surface is more practical.



The quality of the formed monolayer on silicon is critical in determining the interfacial electrical properties and the susceptibility of silicon to oxidation in air and in aqueous solution under oxidative potentials.<sup>65, 66</sup> In particular, higher packing density

leads to a more stable silicon electrode. The size of the molecule in the chemisorbed monolayer dictates the susceptibility of the surface to oxidation by limiting the packing density. We explored two hydroquinone hydroxyl protecting groups, THP (Molecule A) and  $\text{CH}_3$  (Molecule B) (section 4.2.2). THP is removed under milder conditions, and is compatible with using tri-ethylene glycol (TEG, Molecule E) in conjunction with the electroactive molecule (Step II in Scheme 4.2). As a co-component of a monolayer, TEG helps prevent the non-selective binding of cells and proteins (Heath group, unpublished data).<sup>53, 67</sup>

In Figure 4.2 we present representative X-ray photoelectron spectroscopy (XPS) survey scans for the photochemical functionalization of Si(111) and Si(100) with Molecules A and B. All of native oxide has been successfully removed via the wet etch, as evidenced by the absence of O 1s peak in Figure 4.2 (a, b) for (111) and (100), respectively. Furthermore, no Si 2p peaks were observed on high resolution XPS scans between 100 BeV and 104 BeV, which would be expected if traces of  $\text{SiO}_2$  remained. No

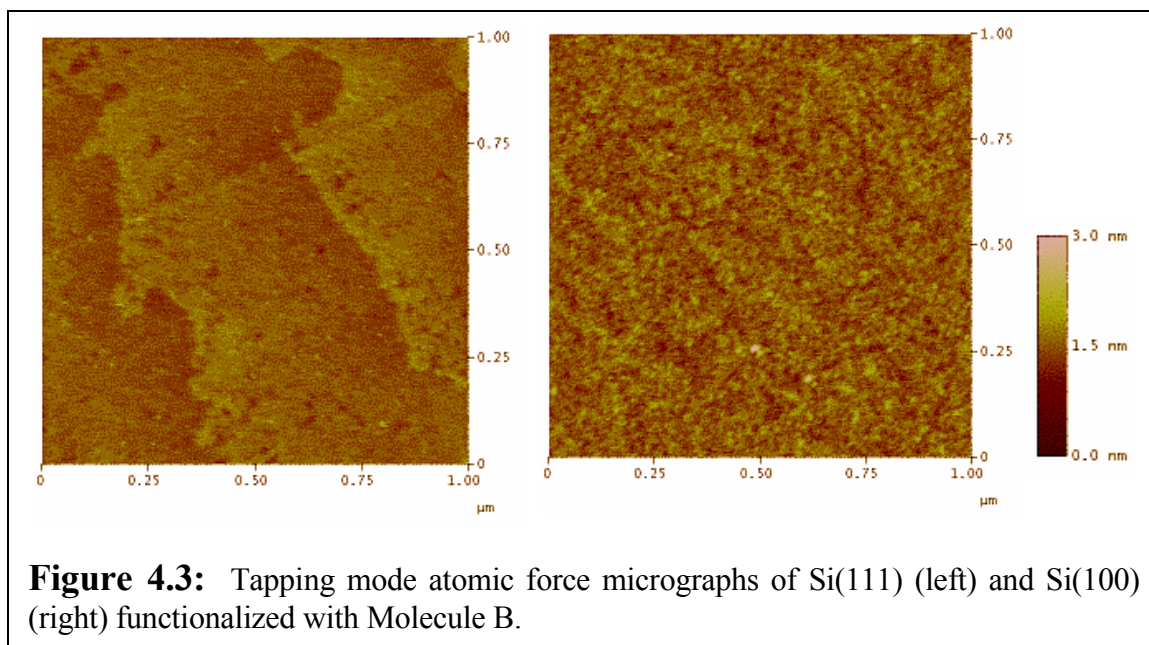


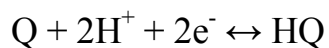
**Figure 4.3:** Tapping mode atomic force micrographs of Si(111) (left) and Si(100) (right) functionalized with Molecule B.

adventitious C 1s peaks at 285 BeV were observed for either (100) or (111) immediately after the wet etch.

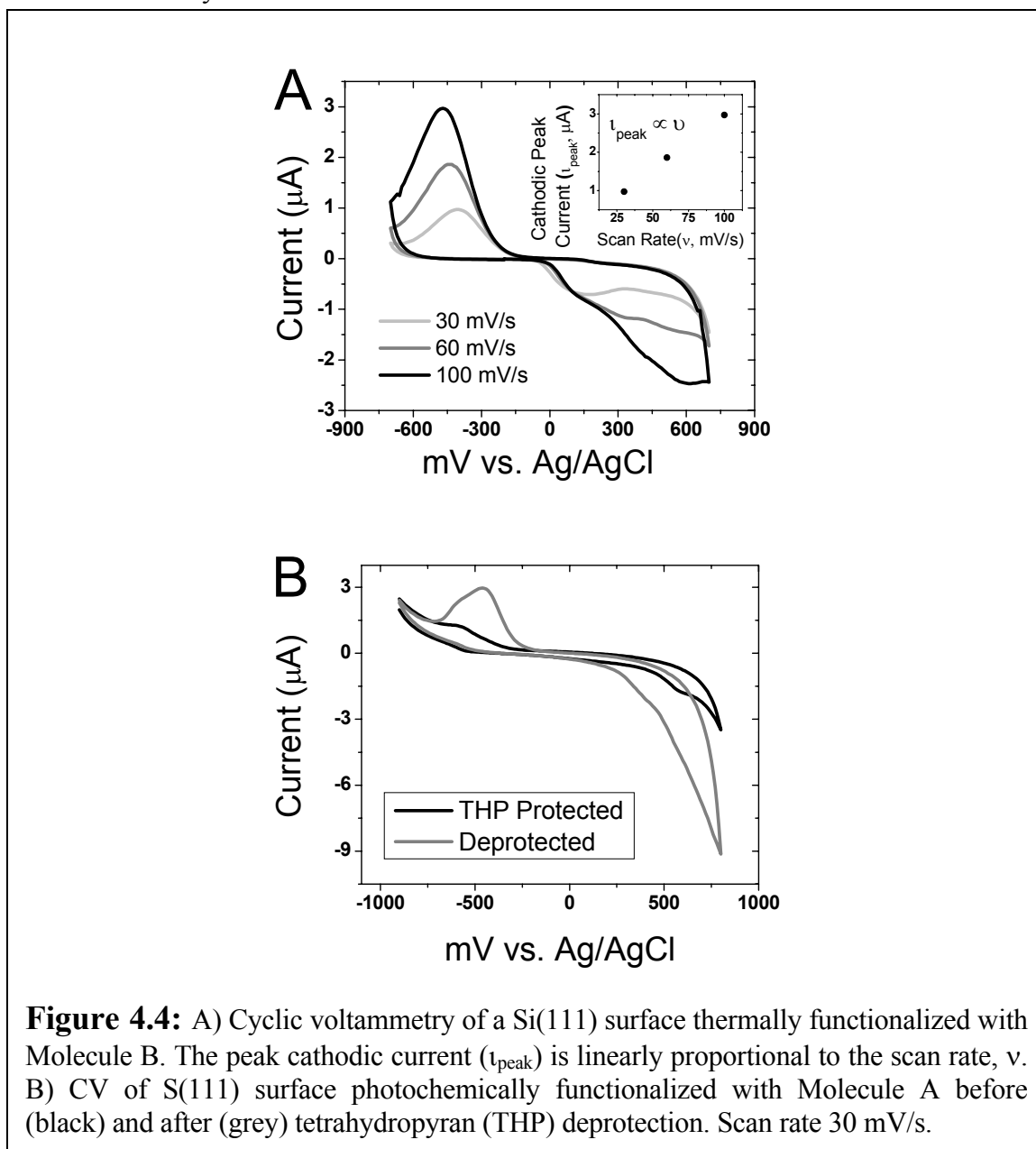
As has been shown previously, atomic force microscopy (AFM) is a useful tool for an assessment of surface stability.<sup>19</sup> Figure 4.3 presents AFM images of Si(111) and Si(100) surfaces functionalized with Molecule B. Atomically flat terraces with monoatomic steps, which resemble those of a well-etched, H-terminated surface,<sup>20</sup> are evident on the (111) substrate. The topography of these surfaces does not change after storage in air or application of small positive potentials (<1V) in aqueous electrolytes. The root mean square (rms) roughness of these surfaces was measured after zooming in on a 0.15 $\mu$ m by 0.15 $\mu$ m area on a single terrace. As expected, the hydroquinone functionalized Si(100) surface is rougher (0.129 $\pm$ 0.006nm) than the Si(111) surface (0.065 $\pm$ 0.004nm). It is likely that the molecular films on (100) are more disordered than those on (111).

Molecule B was synthesized in order to (1) study the effects of molecular size on monolayer stability, and (2) assess the quality of monolayer on silicon prepared by thermally and photochemically induced methods. Molecule A cannot be reacted with silicon surface under thermally induction, since the tetrahydropyran protected group is thermally unstable; however, Molecule B is stable under thermal or photochemical functionalization. Molecule B, however, cannot be used in conjunction with Molecule E since harsh BBr<sub>3</sub> deprotection of methyl groups destroys Molecule E. Figure 4.4A demonstrates the cyclic voltammetry on Si(111) surface functionalized with Molecule B under thermal conditions, 80 °C for 2 hours. We often found that thermal functionalization affords more stable surfaces with better coverage than photochemical functionalization.

Moreover, Figure 4.4A demonstrates that the redox reaction of hydroquinone coupled to silicon surface is diffusion limited.<sup>68</sup> The reaction can be written as follows:



The linear scaling of peak cathodic current with the scan rate indicates that likely the hydrogen diffusion is the limiting rate of the reaction, not the electron transport through the electrode electrolyte interface.



### 4.3.2 Electrochemical Oxidation of Silicon: Organic Monolayer Density and Surface Orientation

We use cyclic voltammetry (CV) to determine the molecular coverage following the deprotection of hydroquinone (Step III of Scheme 4.2). Figure 4.5 illustrates this approach for a monolayer of Molecule B on Si(111) and Si(100), and molecular coverage together with contact angle measurements are presented in Table 4.1. Coverage was obtained by integrating the cathodic peak after all of the surface molecules were converted to the benzoquinone form on a first oxidation sweep to at least 0.6V and then cycled back to the hydroquinone form. A complete conversion to benzoquinone was achieved at potentials above 0.6V because the integrated current plateaus at that value. To correct for non-Faradaic processes, all samples were cycled once at the beginning of the measurement from an open circuit potential to -700mV. The charge obtained from the integration of that cycle was then subtracted from the integrated cathodic peak. The deprotection of the hydroquinone hydroxyl groups is accompanied by a decrease in the static contact angle of 13° to 20°. This decrease in contact angle was reached within 1.5 and 2 hours during the deprotection step for Molecules A and B, respectively, indicating that the deprotection was complete by this time. Complete deprotection eliminates the possibility of underestimating the molecular coverage. Figure 4.4B demonstrates the CV of Si (111) surface functionalized with Molecule A before and after THP deprotection. As expected, the emergence of the reduction peak can only be observed after the hydroxyl deprotection.

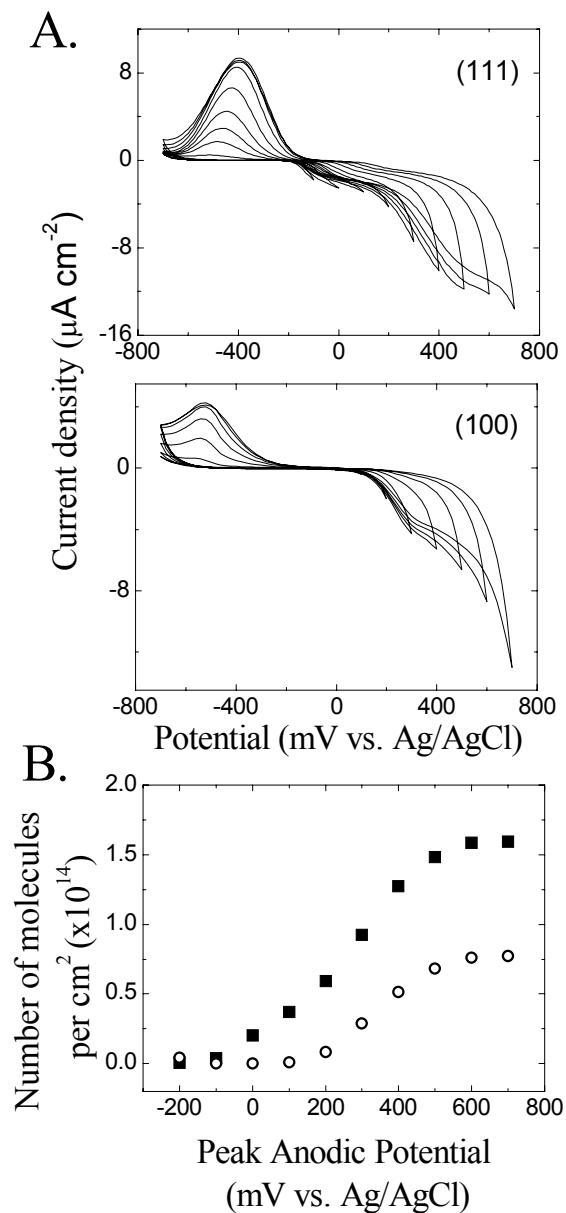


**Figure 4.5:** Measurements of the coverage of Molecule B on Si(111) and Si(100) by cyclic voltammetry (CV). A) Si(111) (top) and Si(100) (bottom): CV scans with increasing peak anodic potential at a scan rate of 50 mV/sec. B) Coverage of electroactive molecules on Si(111) (■) and Si(100) (○) obtained by integrating the reduction peak. The electrolyte was Dulbecco's Phosphate Buffered Saline (pH 7.4).

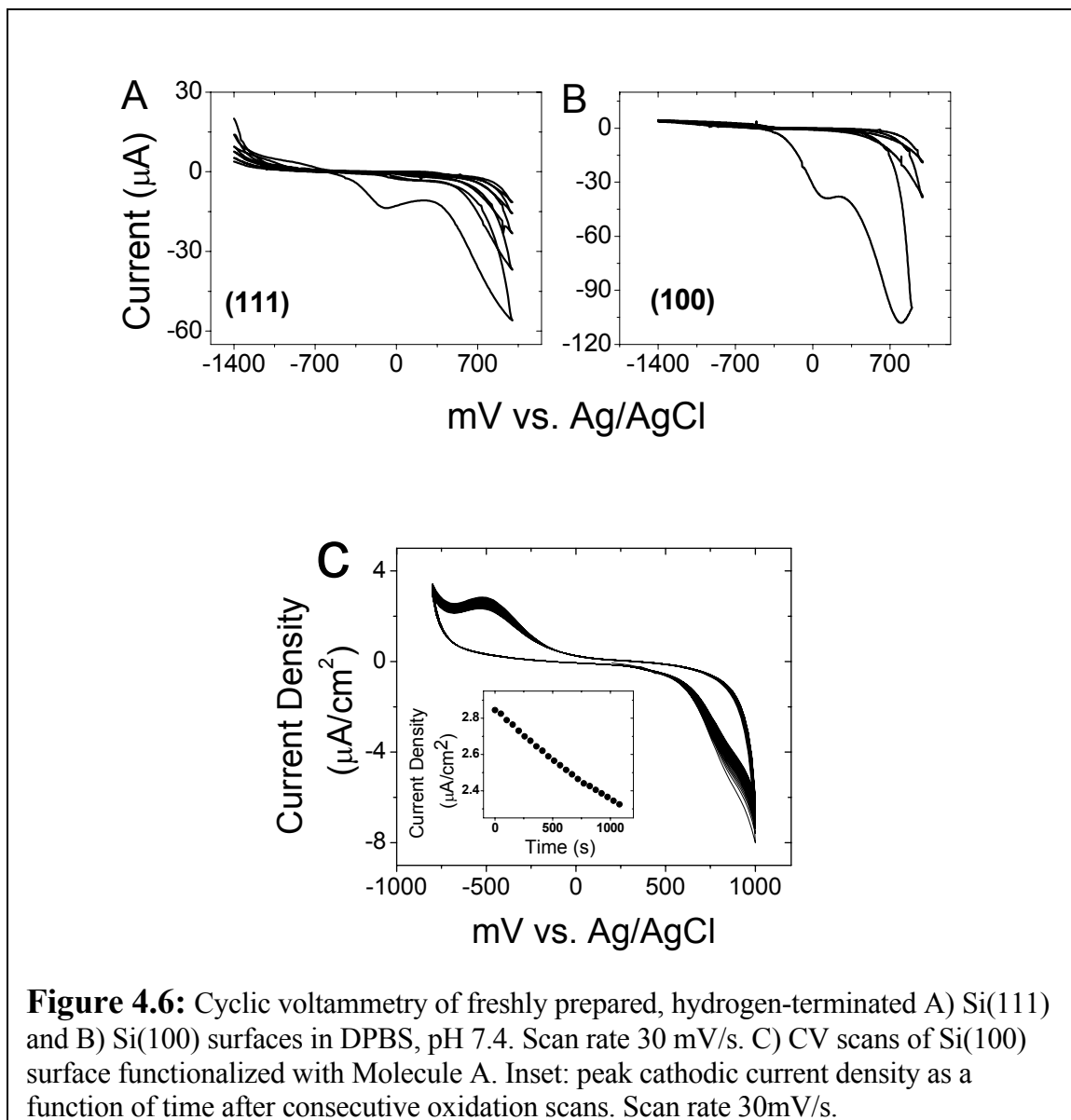
No difference in contact angles was detected between monolayers of Molecules A and B for the same surface. However, comparing (111) and (100) reveals that while the contact angle is similar for Molecules A and B prior to deprotection, both monolayers exhibit a 5° to 7° higher contact angle on (100) after deprotection.

Hydroquinone protecting group	Static contact angle /° (before and after –OH deprotection)				Coverage (# molecules/Å <sup>2</sup> )	
	Si(111)		Si(100)		Si (111)	Si(100)
	Before	After	Before	After		
CH <sub>3</sub> (Mol. B)	73.7±0.8	54.6±1.4	74.1±0.1	61.1±2.0	0.23±0.01	0.17±0.02
THP (Mol. A)	72.0±1.3	53.2±1.2	72.5±0.6	58.7±1.8	0.20±0.01	0.11±0.005

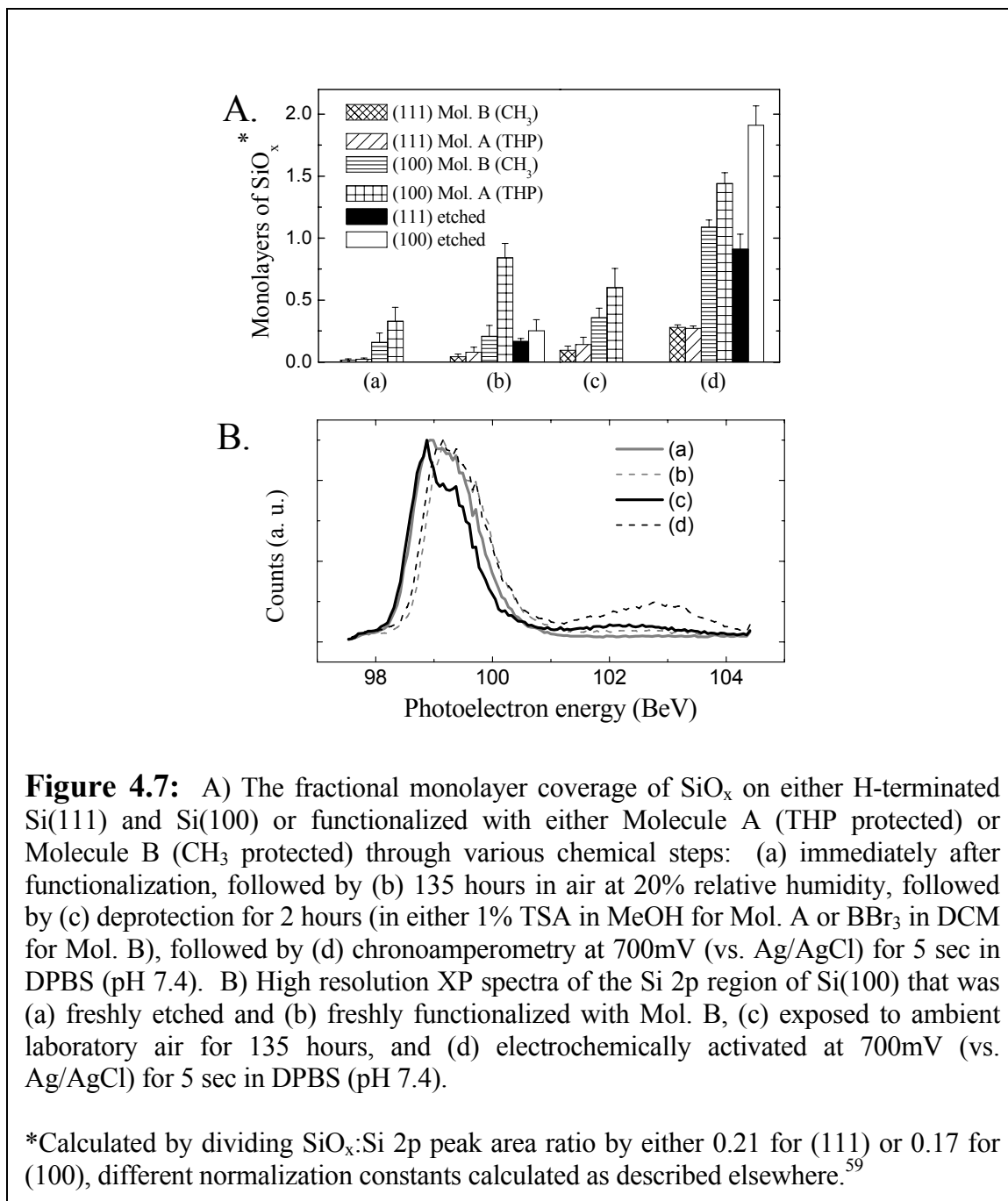
**Table 4.1:** Monolayer characterization, separated by substrate and by hydroquinone protecting group. The coverage data has been normalized to per silicon atom, taking into consideration the difference in surface densities of Si(111) and Si(100).

As expected, the coverage of Molecules A and B on Si(100) is lower than on Si(111). Table 4.1 also demonstrates that molecular size plays less of a role on the packing density on Si(111): molecules A and B exhibit similar coverage on (111) but quite different coverage on (100).

Due to lower surface density of atoms, Si(100) is more susceptible to oxidize in an electrolyte solution. Figure 4.6 presents CV scans of an electrochemical oxidation of freshly prepared, hydrogen terminated Si(100) and Si(111) surfaces. The electrode areas are identical, so the current density of Si(100) oxidation is larger, corresponding to a more extensive oxidation. Moreover, Si(100) functionalized with Molecule A is progressively oxidized by cycling between two forms of the molecule, as evidenced by the linear drop in the peak cathodic current in Figure 4.5. On Si(111) surface, such drop in current is not



evident, arguing that the molecule itself is stable after multiple CV scans. Figure 4.7 trace is the silicon oxidation of H-terminated and organically functionalized (111) and (100) substrates through various processes, including the formation of the molecular monolayer, incubation in air at 20% relative humidity, deprotection of the monolayer to form the hydroquinone, and electrochemical oxidation to form the benzoquinone. The method used to quantify the overlying oxide is presented in greater details in section 4.2.4.



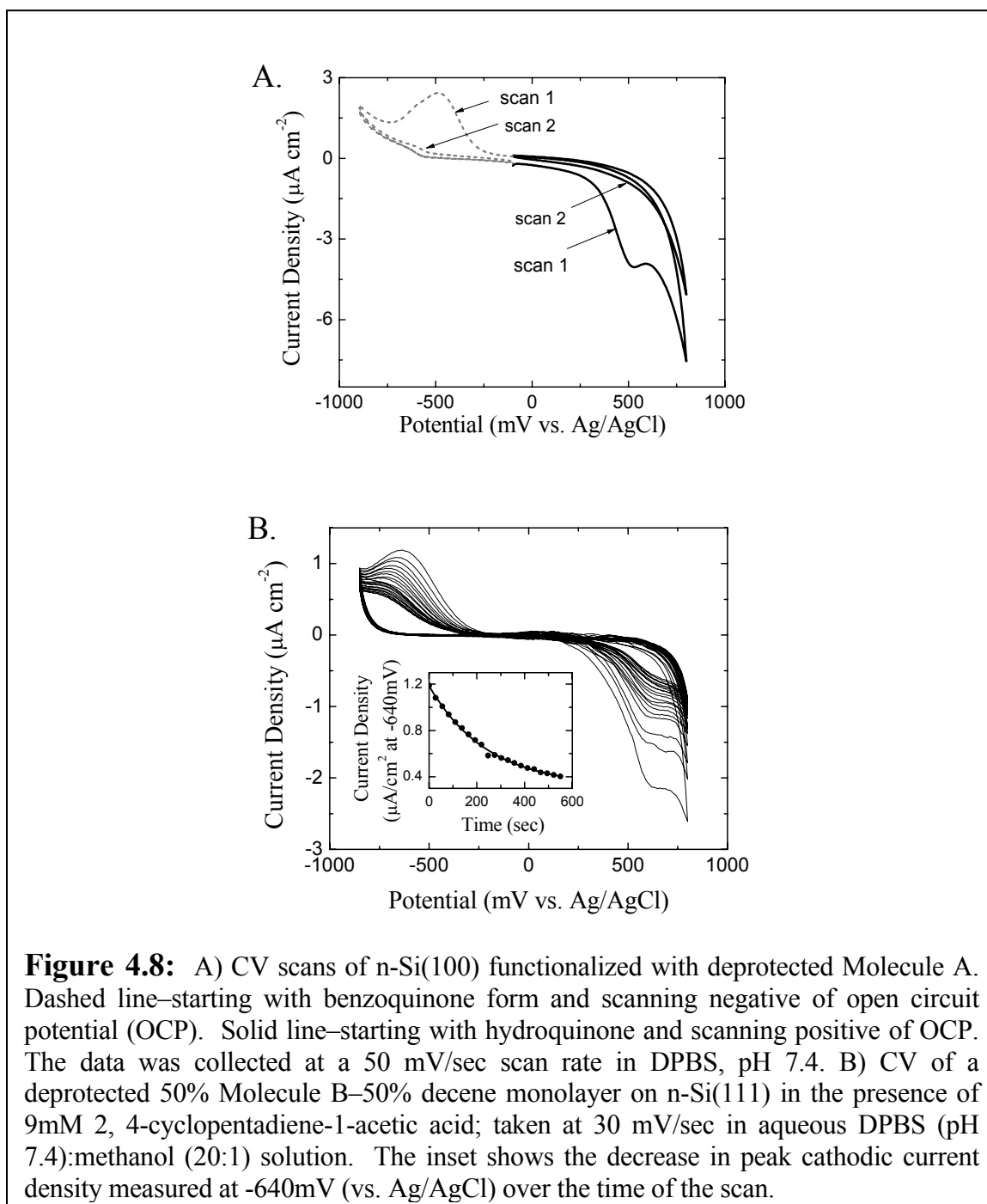
We assumed that the organic monolayer causes minimal attenuation of the photoelectrons, although it is possible that the data presented in Figure 4.7 is slightly underestimated because of this assumption. H-terminated and functionalized Si(100) consistently demonstrate higher degree of oxidation than Si(111), consistent with the literature.<sup>62-64</sup> In

addition, substrates with monolayers of Molecule A exhibit consistently higher levels of oxide than those functionalized with Molecule B. Our data indicate that the functionalized (100) surfaces are oxidized the same amount as H-terminated Si when stored at room temperature and 20% relative humidity, while Si(111) show extreme chemical stability. We have observed that after eight months of storage, less than half of an equivalent SiO<sub>2</sub> monolayer exists on functionalized Si(111) samples. Curiously, Si(100) functionalized with Molecule A showed more oxide after incubation in air than H-terminated Si(100). This may have resulted from trace water present in the Molecule A solution. For both (100) and (111) surfaces, a negligible change was observed in the amount of oxide grown during the deprotection steps of either Molecule A or B.

### **4.3.3 Diels-Alder Reaction and Michael Addition on Silicon**

Keeping the immobilized biological molecules in a functional state is absolutely necessary for the development of any sensor array, including NW arrays. One corresponding constraint for this chemistry is that the biological probe attachment step and sensing must be done in an aqueous electrolyte. Alkyl monolayers formed onto H-terminated Si surfaces have been shown to reduce anodic oxidation in aqueous media,<sup>65, 66</sup> however, the quality of the monolayer again plays a critical role here. Figure 4.7 clearly demonstrates that a short pulse of a small positive potential, although sufficient to oxidize all surface hydroquinone molecules (Figure 4.8A), only slightly oxidizes the functionalized Si(111), compared with the non-functionalized substrate. The difference is less pronounced for the case of Si(100). We have observed a direct correlation between the packing density and the amount of anodic oxidation of functionalized silicon in phosphate buffer at pH 7.4. Consistent with the packing density data from Table 4.1, molecular size

plays an insignificant role in anodic oxidation of Si(111), while Si(100) functionalized with Molecule A is oxidized more extensively than that functionalized with Molecule B.



The oxidation and reduction peaks of hydroquinone on medium doped ( $\sim 10^{18} \text{ cm}^{-3}$ )

n-type silicon are observed at approximately 350mV and -500mV (vs. Ag/AgCl) on an

initial CV scan. CV measurements on very similar molecules formed as SAMs on Au surfaces reveal the oxidation peak at approximately 300mV and the corresponding reduction peak at -150mV.<sup>45</sup> The redox potentials of hydroquinone/benzoquinone on the functionalized Si electrodes, however, depend upon the quality of the organic monolayer and shift to larger overpotentials as oxidation of the substrate adds to the surface impedance. Figures 4.5A and 4.6C demonstrate a small decrease in current density with consecutive CV scans and a shift of the anodic peak to higher overpotentials. Consistent with the data reported elsewhere,<sup>66</sup> the open circuit potential (OCP) of alkylated silicon electrodes used in this study was shifted to between -100 and -200mV (Figure 4.8A). Silicon oxidation in an aqueous electrolyte causes an accumulation of electrons on the Si surface, shifting the OCP to negative overpotentials.

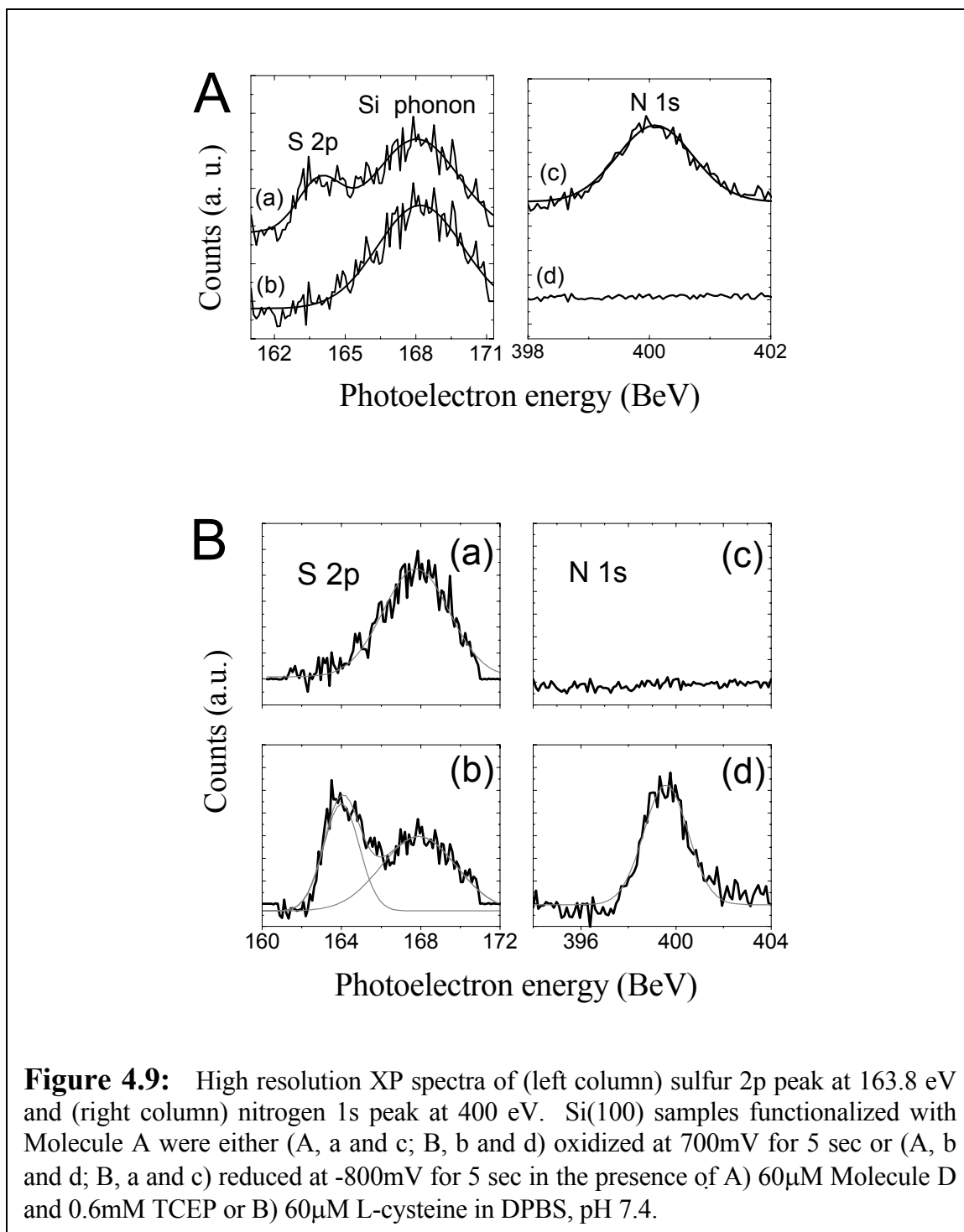
The effects of monolayer composition and surface functional groups on the kinetics of Diels-Alder interfacial reactions have been clearly demonstrated for the case of Au substrates.<sup>45</sup> Figure 4.8A shows that the monolayer is completely oxidized and reduced at 800mV and -900mV, respectively. Furthermore, both reduced and oxidized forms of the molecule are quite stable. The relaxation rate of *p*-benzoquinone is slower than either the Michael addition or Diels-Alder reaction (data not shown). Therefore, it is sufficient to pulse the monolayer for a few seconds without applying either subsequent pulses or holding the Si electrode at anodic potentials. An attractive aspect of using the hydroquinone and Diels-Alder chemistry for spatially selective biomolecular attachment is that the redox reaction is electrochemically reversible, which allows for an accurate determination of reaction rates using CV. Figure 4.8B shows a CV trace for a mixed monolayer in the presence of 9mM 2,4-cyclopentadiene-1-acetic acid. To increase the

packing density and to minimize anodic oxidation, mixed monolayers of electroactive molecule combined with 1-decene were used. In general, using short unsubstituted alkenes in conjunction with hydroquinone leads to denser packing of the monolayer, which renders the underlying substrate less prone to oxidation. The rate of this Diels-Alder reaction could be obtained by fitting the decrease in peak cathodic current to the following equation<sup>45</sup>

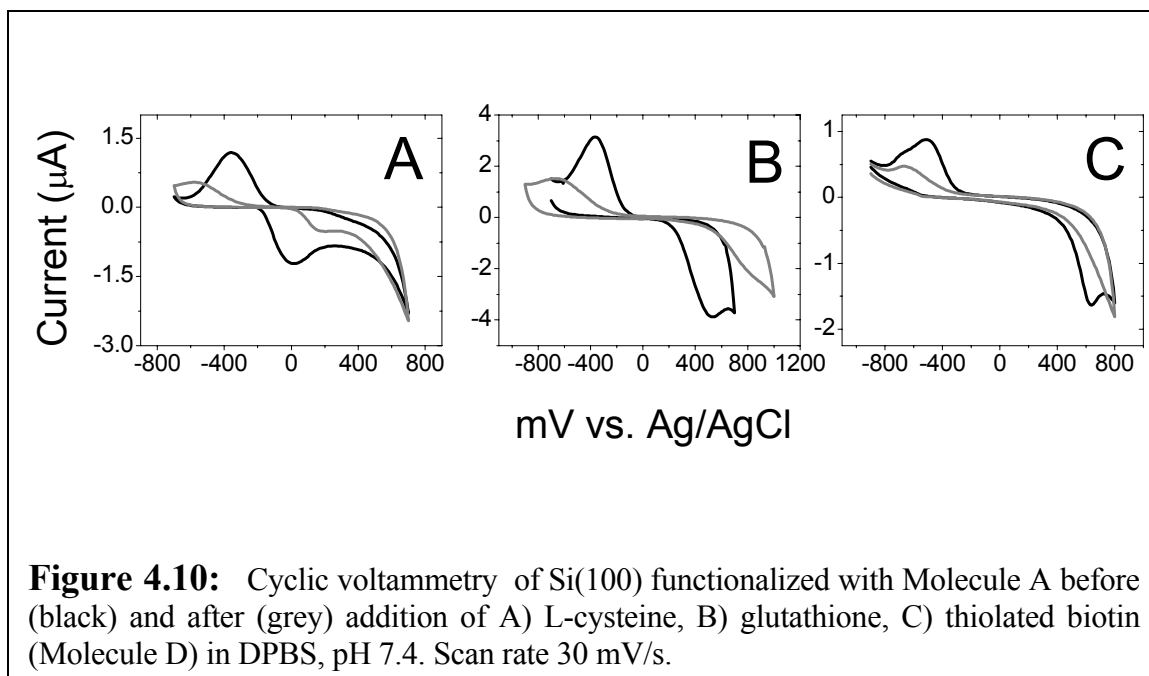
$$I_t = I_f + (I_o - I_f)\exp^{-\kappa t}$$

Here,  $\kappa=0.005 \text{ s}^{-1}$ , which is about five times faster than the rate of addition of cyclopentadiene of equal concentration reported on Au electrodes.<sup>45</sup> The cathodic current was evaluated to determine the reaction rates because the current associated with the oxidation of the Si surface is convoluted into the anodic peak, as is clearly visible in Figures 4.5 and 4.6C.

We also demonstrated Michael addition of thiolated molecules to 1,4-benzoquinone as an alternative coupling chemistry (Step V of Scheme 4.2) that is not available for hydroquinones bound to Au surfaces. This chemistry is advantageous because the native cysteines of antibodies or other proteins could potentially be utilized,<sup>51, 69</sup> and thiol-terminated nucleic acids are commercially available. The high-resolution XPS data presented in Figure 4.9 (A, B) reveal clear S 2p and N 1s peaks of an oxidized monolayer on Si(100) which was reacted with thiol-terminated biotin (reduced Molecule D) or cysteine, respectively. A reduced hydroquinone monolayer that was taken through the same chemical exposures exhibited no evidence of sulfur or nitrogen presence. Other small, thiol-containing molecules such as L-cysteine (Figure 4.9B) and glutathione were also reacted with the oxidized monolayer.<sup>50, 70</sup> Figure 4.10 demonstrates the cyclic voltammetry of hydroquinone on silicon before and after addition of thiol-containing



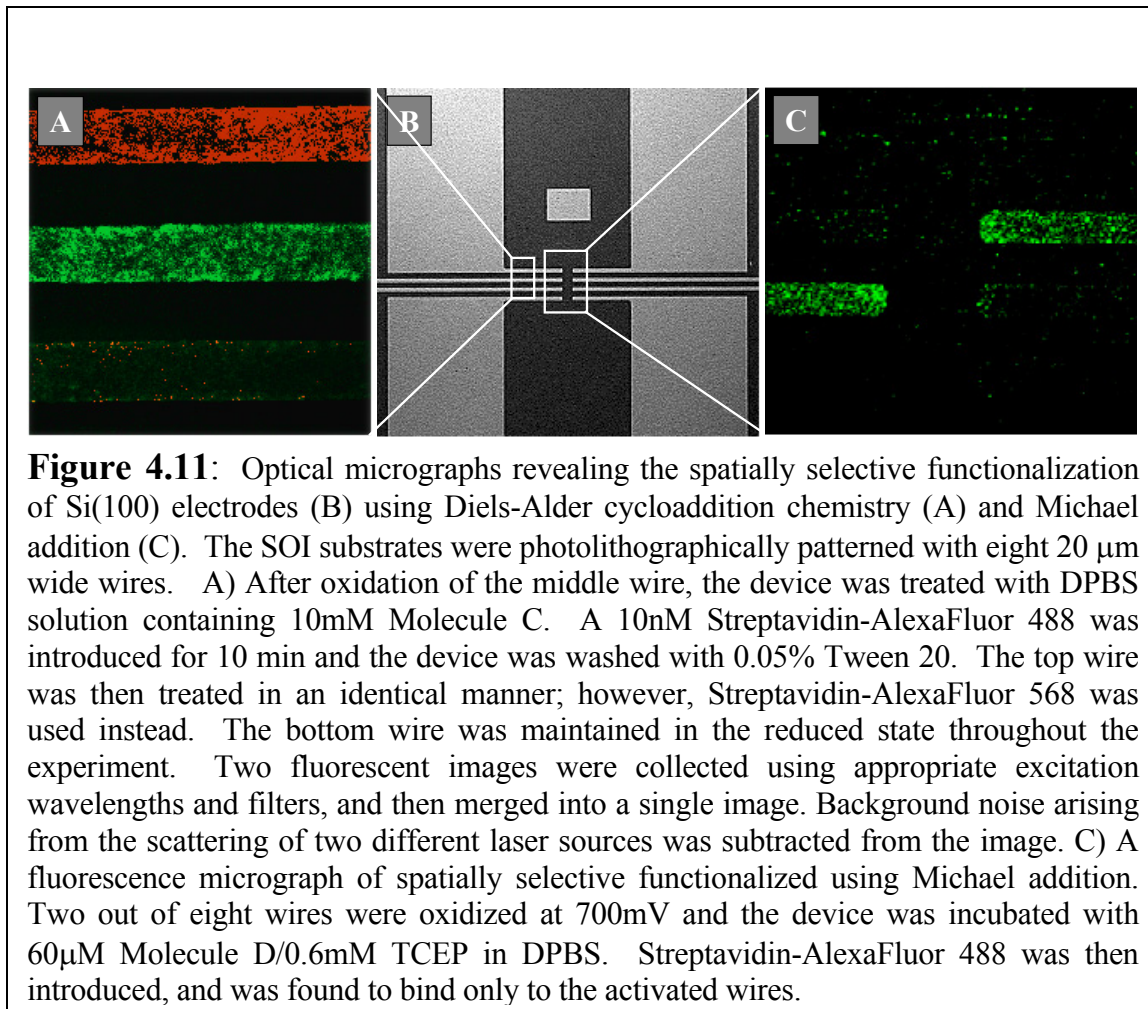
molecules. In each case, the oxidation and reduction peaks were diminished and shifted to higher overpotentials. The covalent attachment of molecules was validated with XPS (Figure 4.9).



#### 4.4 Selective Functionalization of Silicon Micro- and Nanowires

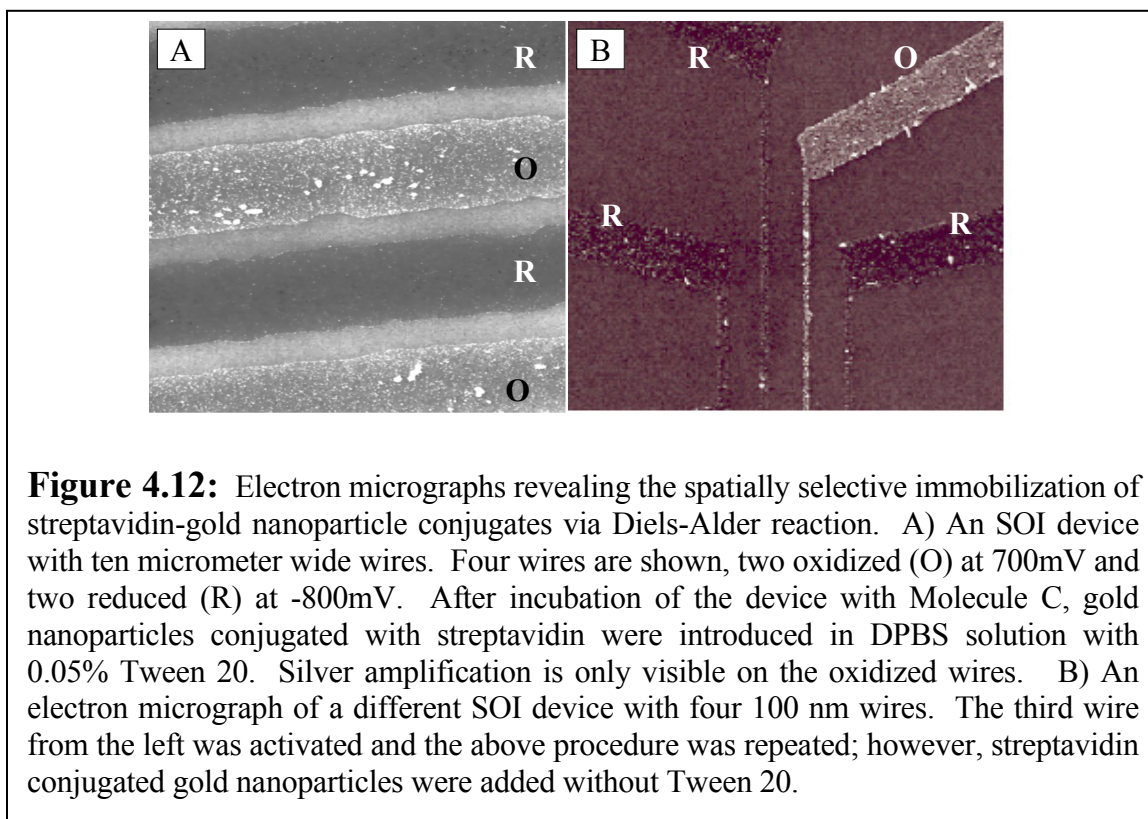
The Scheme 4.2 strategy could be used to selectively functionalize micro- and nanostructures patterned on silicon-on-insulator (SOI) substrates and to subsequently immobilize proteins onto selected electrodes (Figures 4.11 and 4.12). Microwires were patterned using conventional photolithography, and nanowires were patterned using electron beam lithography. Following the steps outlined in Scheme 4.2, a potential of 700mV (vs. Ag/AgCl) was applied to specific wires. All of the wires were immersed into the solution containing either Molecule C (Figures 4.11A and 4.12) or reduced Molecule D (Figure 4.11C), followed by the introduction of a fluorescent dye-streptavidin conjugate (Figure 4.11) or gold nanoparticles functionalized with streptavidin (Figure 4.12). Figure 4.11A demonstrate that this approach can be used to construct a protein library of two elements.

After a particular protein was coupled to one silicon electrode, biofunctionalization of an additional electrode on the same device did not affect the previously functionalized electrode. It is thus apparently possible to saturate all the active sites on a given silicon electrode and to prevent cross-functionalization between two electrically isolated



electrodes. However, it was necessary to clean the surfaces by sonication in 0.05% Tween 20 solution after every addition of protein to remove nonselectively bound proteins, and this step may explain the dark patches appearing on the electrodes in Figure 4.11. The sites vacated by leaving proteins may not be suitable for further molecular attachment. It was possible to assess the degree of nonspecific adsorption on a given electrode by recording the current density during the oxidation. While the current densities upon the oxidation of

the first set of electrodes on a device did not vary, activation of the subsequent electrodes after the device had already been exposed to protein consistently exhibited lower current densities. Furthermore, the electrode edges almost always exhibited more non-specific fluorescent signal than did the central portions. This may arise from sharper field gradients at those edges.



We extended this approach to the selective biopassivation of 100 nm wide, 50 nm high nanowires (patterned using e-beam lithography) that were spaced too closely together (0.3  $\mu\text{m}$  pitch) to easily resolve using fluorescence microscopy. Therefore, we utilized the well-established  $\text{Ag}^+$  amplification scheme<sup>71</sup> to assess fidelity of the biopassivation on those nanostructures, and the results are shown in Figure 4.12. In this scheme, streptavidin conjugated gold nanoparticles are bonded to the electroactive site, and a silver layer is grown onto the Au particles. The nanowires exhibited more nonspecific binding than the

microwires. As noted above, the edges of the microwires exhibited more non-specific binding, and this affect may be exacerbated for the case of nanowires. In addition, as Figure 4.12 demonstrates, it was possible to essentially eliminate the nonspecific binding on the microwires by including Tween 20 detergent with the streptavidin. Therefore, even without the use of TEG or other chemical approaches designed to prevent non-specific binding, this method can be used for spatially selective immobilization of proteins.

## 4.5 Discussion

### 4.5.1 Mixed Monolayers and Biofouling Minimization

We describe an electrochemical method to selectively functionalize silicon micro- and nanoelectrodes utilizing Diels-Alder and Michael additions. Such route of selective molecular immobilization should be especially valuable for the biopassivation of ultra dense arrays of electronically addressable silicon nanowires<sup>72</sup> (chapter 2) or other nanostructures such as nanomechanical sensors.<sup>73, 74</sup> This method avoids the spatial limitations of alternative techniques such as inkjet spotting, or the alignment and registry limitations of dip-pen lithography. While the selectivity of this process, as shown in

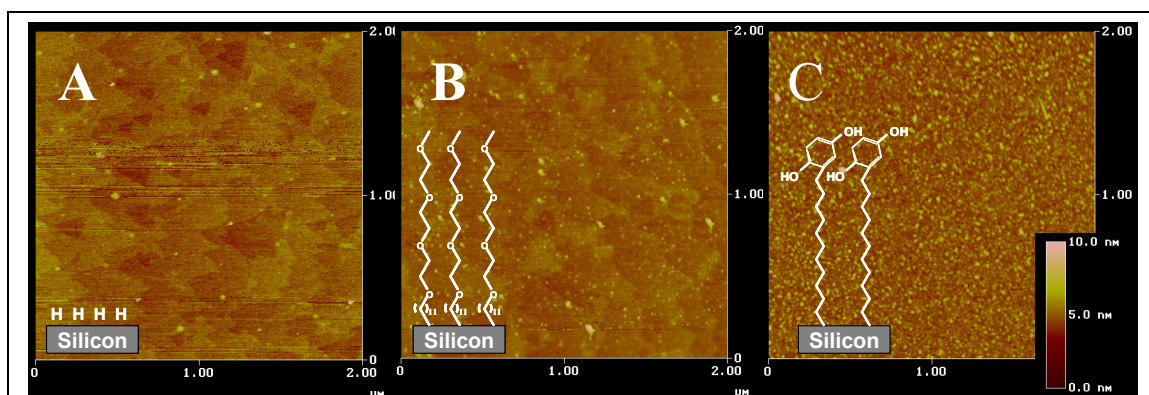


**Figure 4.13:** Tapping mode atomic force micrographs of Si(111) surface A) hydrogen terminated, B) functionalized with Molecule E, or C) functionalized with Molecule A, after exposure to 90nM streptavidin solution.

Figures 4.11 and 4.12, is evident, it can be substantially improved beyond the results presented here. For example, mixed monolayers incorporating TEG units will minimize nonspecific adsorption of proteins<sup>53</sup> and improve the selectivity of this approach. Our preliminary results on such mixed monolayers demonstrate that the high packing density

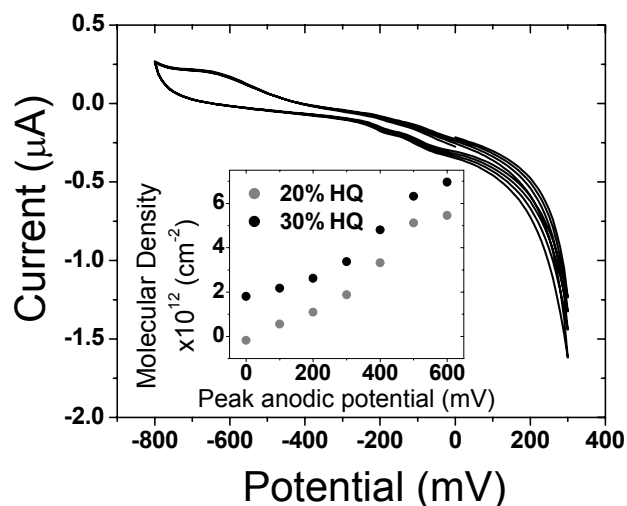


**Figure 4.14:** Cyclic voltammety of mixed 20% (v/v) hydroquinone (Molecule A): 80% tri(ethylene glycol) (TEG, Molecule E) monolayer on Si(111) in DPBS, pH 7.4. Scan rate 30 mV/s. Inset: density of hydroquinone (HQ) molecules in 20% HQ/80% TEG (grey) and 30% HQ/70% TEG (black) monolayers as a function of maximum anodic potential reached.

of TEG terminated alkanes (Molecule E) yields more stable silicon electrodes than the ones functionalized only with hydroquinone-terminated alkanes. Figure 4.13 demonstrates the resistance of such surfaces to protein biofouling. Biofouling does not only cause significant noise in electronic sensing, but will most likely be a hindrance in building a large element library with the electrochemical method described above. However, mixed monolayers composed of the electroactive molecules and tri(ethylene glycol) will most likely decrease the problem of biofouling, while further stabilizing the

silicon surface. The cyclic voltammetry on Si(111) surface with such mixed monolayer is shown in Figure 4.14. As is evident from the presence of a reversible reduction peak, the hydroquinone moiety remains functional at low densities, which can be tuned to yield sufficient selective attachment of probe molecules while minimizing the non-specific binding. Furthermore, electrode stability may be substantially improved by modulating the doping levels, or utilizing p-type Si rather than the highly doped n-type substrates used in this study.<sup>62, 63</sup> Extending this approach to nanowire circuits (Figure 4.15), however, is going to present a number of challenges, not the least of which will involve analytical methods, since most of the techniques utilized here are not easily translated to high density nanowire circuits.

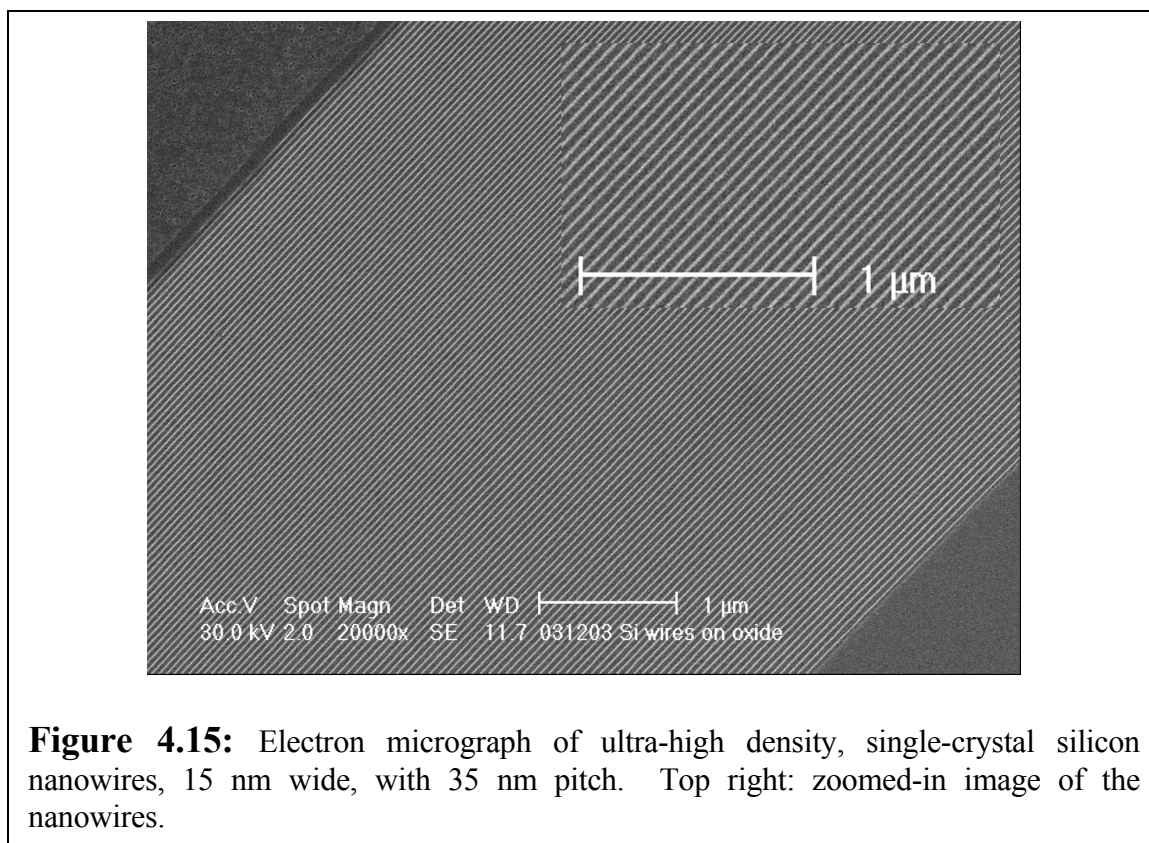
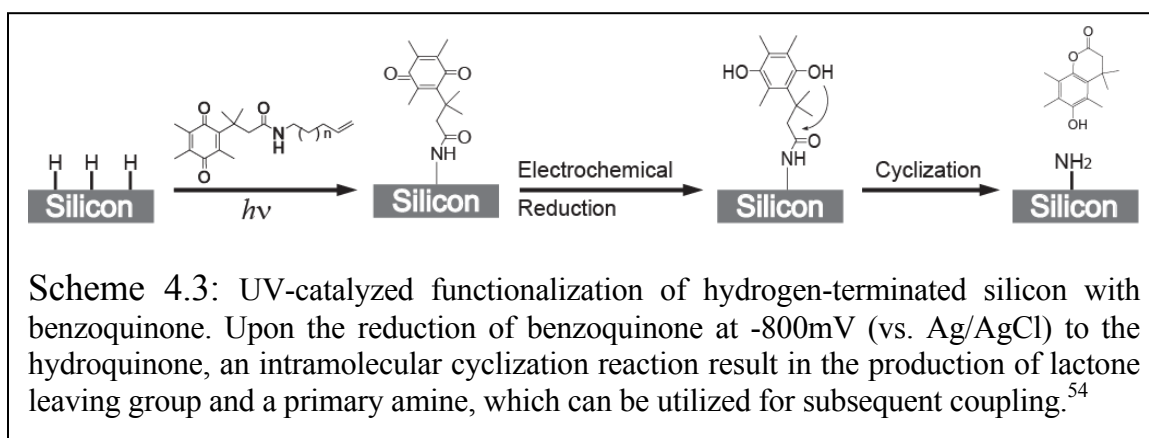


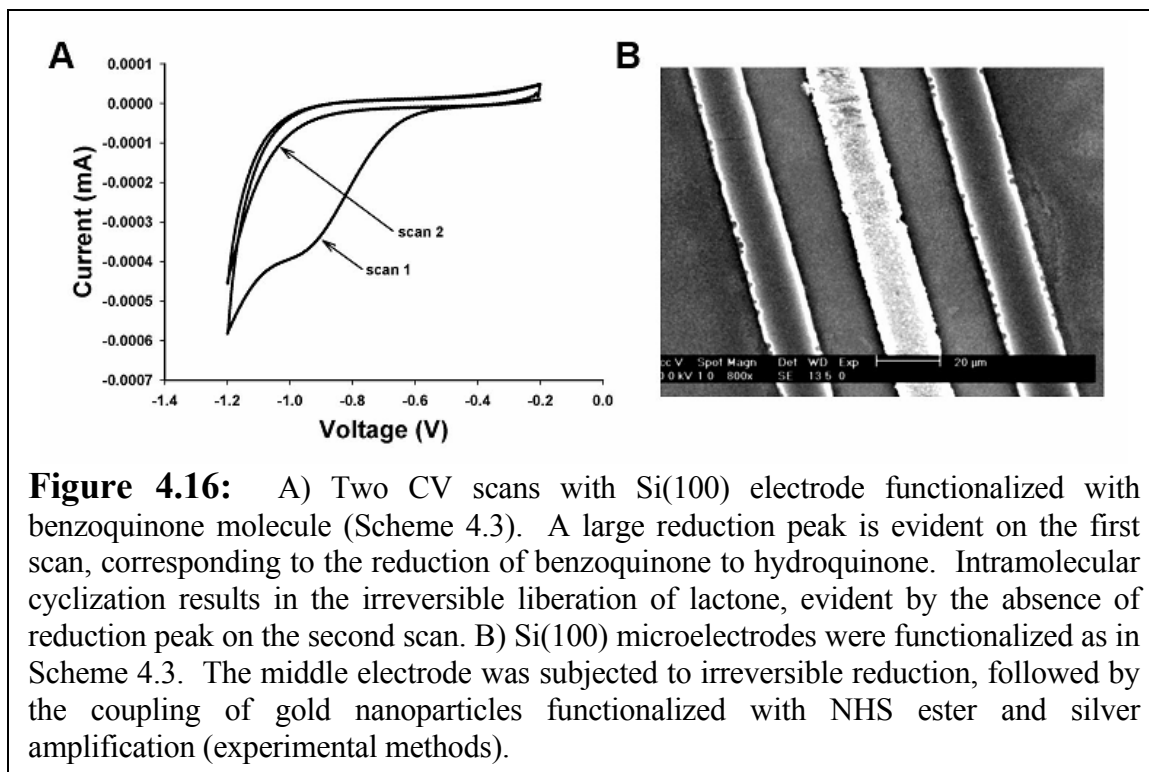
**Figure 4.15:** Electron micrograph of ultra-high density, single-crystal silicon nanowires, 15 nm wide, with 35 nm pitch. Top right: zoomed-in image of the nanowires.

### 4.5.2 Reductive Functionalization

As described above, electrochemical conversion of hydroquinone to *p*-benzoquinone causes appreciable oxidation of silicon surfaces, and may play an adverse role in nanowire electrical sensing.<sup>5</sup> Therefore, our group has embarked on finding alternative strategies of spatially selective, electrochemical functionalization of silicon. In particular, an electrochemical method which relies on the reductive conversion of the electroactive molecule (Scheme 4.3) to its active form will be particularly beneficial in avoiding oxidative damage to the nanowire surface.<sup>54</sup> Scheme 4.3 outlines the steps in



electrochemically converting a benzoquinone molecule to a primary surface amine via an intramolecular cyclization and liberation of a lactone group. The electrochemical reduction is irreversible, as demonstrated in Figure 4.16A. Surface amine is a general group which can be utilized for subsequent functionalization with a variety of molecules and biological probes. We employed this chemistry to demonstrate a spatially selective coupling of gold nanoparticles functionalized with N-hydroxysuccinimidyl ester (NHS ester) to the surface amines generated via a reductive electrochemical deprotection (Figure 4.16B).



Recent developments in spatially selective electrochemical functionalization indicate that this field is of interest due to its relevance in a wide variety of applications.<sup>75-80</sup> This chapter addresses some important issues pertaining to the passivation of hydrogen terminated silicon with electroactive molecules, with emphasis on obtaining the most stable surfaces which are resistant to oxidation in air and in aqueous media. Parameters such as molecular size, monolayer density, and crystal orientation of silicon surface affect the silicon electrode stability in a profound way. We further demonstrate that individually addressed silicon micro- and nanowires may be utilized to create an electrochemically encoded protein library of an arbitrary density.<sup>81</sup> Direct surface passivation of silicon affords several important advantages. First, reactions involving immobilized electroactive molecules may only be carried out at low voltages ( $-1V < \text{voltage} < 1V$ ) if the native oxide

of silicon is replaced with a short organic monolayer. Second, directly passivated silicon nanowires are much more effective biological sensors in high ionic strength solution.<sup>72</sup>

## Bibliography

1. Fodor, S. P. A.; Read, J. L.; Pirrung, M. C.; Stryer, L.; Lu, A. T.; Solas, D., Light-directed, spatially addressable parallel chemical synthesis. *Science* **1991**, 251, (4995), 767-773.
2. MacBeath, G.; Schreiber, S. L., Printing proteins as microarrays for high-throughput function determination. *Science* **2000**, 289, (5485), 1760-1763.
3. Lee, K. B.; Park, S. J.; Mirkin, C. A.; Smith, J. C.; Mrksich, M., Protein nanoarrays generated by dip-pen nanolithography. *Science* **2002**, 295, (5560), 1702-1705.
4. Cui, Y.; Wei, Q. Q.; Park, H. K.; Lieber, C. M., Nanowire nanosensors for highly sensitive and selective detection of biological and chemical species. *Science* **2001**, 293, (5533), 1289-1292.
5. Bunimovich, Y. L.; Shin, Y. S.; Yeo, W. S.; Amori, M.; Kwong, G.; Heath, J. R., Quantitative real-time measurements of DNA hybridization with alkylated nonoxidized silicon nanowires in electrolyte solution. *J. Am. Chem. Soc.* **2006**, 128, (50), 16323-16331.
6. Melosh, N. A.; Boukai, A.; Diana, F.; Gerardot, B.; Badolato, A.; Petroff, P. M.; Heath, J. R., Ultrahigh-density nanowire lattices and circuits. *Science* **2003**, 300, (5616), 112-115.
7. Beckman, R. A.; Johnston-Halperin, E.; Melosh, N. A.; Luo, Y.; Green, J. E.; Heath, J. R., Fabrication of conducting Si nanowire arrays. *J. Appl. Phys.* **2004**, 96, (10), 5921-5923.
8. Wang, D. W.; Sheriff, B. A.; Heath, J. R., Silicon p-FETs from ultrahigh density nanowire arrays. *Nano Lett.* **2006**, 6, (6), 1096-1100.
9. Wang, D. W.; Sheriff, B. A.; Heath, J. R., Complementary symmetry silicon nanowire logic: Power-efficient inverters with gain. *Small* **2006**, 2, (10), 1153-1158.
10. Beckman, R.; Johnston-Halperin, E.; Luo, Y.; Green, J. E.; Heath, J. R., Bridging dimensions: Demultiplexing ultrahigh-density nanowire circuits. *Science* **2005**, 310, (5747), 465-468.
11. Buriak, J. M., Organometallic chemistry on silicon and germanium surfaces. *Chem. Rev.* **2002**, 102, (5), 1271-1308.
12. Sieval, A. B.; Linke, R.; Zuilhof, H.; Sudholter, E. J. R., High-quality alkyl monolayers on silicon surfaces. *Adv. Mater.* **2000**, 12, (19), 1457-1460.
13. Wayner, D. D. M.; Wolkow, R. A., Organic modification of hydrogen terminated silicon surfaces. *J. Chem. Soc., Perkin Trans. 2* **2002**, (1), 23-34.
14. Sung, M. M.; Kluth, G. J.; Yauw, O. W.; Maboudian, R., Thermal behavior of alkyl monolayers on silicon surfaces. *Langmuir* **1997**, 13, (23), 6164-6168.
15. Li, Q. L.; Mathur, G.; Homsji, M.; Surthi, S.; Misra, V.; Malinovskii, V.; Schweikart, K. H.; Yu, L. H.; Lindsey, J. S.; Liu, Z. M.; Dabke, R. B.; Yasseri, A.; Bocian, D. F.; Kuhr, W. G., Capacitance and conductance characterization of ferrocene-containing self-assembled monolayers on silicon surfaces for memory applications. *Appl. Phys. Lett.* **2002**, 81, (8), 1494-1496.
16. Royea, W. J.; Juang, A.; Lewis, N. S., Preparation of air-stable, low recombination velocity Si(111) surfaces through alkyl termination. *Appl. Phys. Lett.* **2000**, 77, (13), 1988-1990.

17. Hu, M. H.; Noda, S.; Okubo, T.; Yamaguchi, Y.; Komiyama, H., Structure and morphology of self-assembled 3-mercaptopropyltrimethoxysilane layers on silicon oxide. *Appl. Surf. Sci.* **2001**, 181, (3-4), 307-316.
18. Lenigk, R.; Carles, M.; Ip, N. Y.; Sucher, N. J., Surface characterization of a silicon-chip-based DNA microarray. *Langmuir* **2001**, 17, (8), 2497-2501.
19. Boukherroub, R.; Morin, S.; Bensebaa, F.; Wayner, D. D. M., New synthetic routes to alkyl monolayers on the Si(111) surface. *Langmuir* **1999**, 15, (11), 3831-3835.
20. Zhang, L. Z.; Li, L. Y.; Chen, S. F.; Jiang, S. Y., Measurements of friction and adhesion for alkyl monolayers on Si(111) by scanning force microscopy. *Langmuir* **2002**, 18, (14), 5448-5456.
21. Linford, M. R.; Chidsey, C. E. D., Alkyl monolayers covalently bonded to silicon surfaces. *J. Am. Chem. Soc.* **1993**, 115, (26), 12631-12632.
22. Linford, M. R.; Fenter, P.; Eisenberger, P. M.; Chidsey, C. E. D., Alkyl monolayers on silicon prepared from 1-alkenes and hydrogen-terminated silicon. *J. Am. Chem. Soc.* **1995**, 117, (11), 3145-3155.
23. Sieval, A. B.; Demirel, A. L.; Nissink, J. W. M.; Linford, M. R.; van der Maas, J. H.; de Jeu, W. H.; Zuilhof, H.; Sudholter, E. J. R., Highly stable Si-C linked functionalized monolayers on the silicon (100) surface. *Langmuir* **1998**, 14, (7), 1759-1768.
24. Sieval, A. B.; Linke, R.; Heij, G.; Meijer, G.; Zuilhof, H.; Sudholter, E. J. R., Amino-terminated organic monolayers on hydrogen-terminated silicon surfaces. *Langmuir* **2001**, 17, (24), 7554-7559.
25. Boukherroub, R.; Wayner, D. D. M.; Lockwood, D. J.; Canham, L. T., Passivated luminescent porous silicon. *J. Electrochem. Soc.* **2001**, 148, (9), H91-H97.
26. Boukherroub, R.; Wojtyk, J. T. C.; Wayner, D. D. M.; Lockwood, D. J., Thermal hydrosilylation of undecylenic acid with porous silicon. *J. Electrochem. Soc.* **2002**, 149, (2), H59-H63.
27. Terry, J.; Mo, R.; Wigren, C.; Cao, R. Y.; Mount, G.; Pianetta, P.; Linford, M. R.; Chidsey, C. E. D., Reactivity of the H-Si (111) surface. *Instrum. Methods Phys. Res., Sect. B* **1997**, 133, (1-4), 94-101.
28. Terry, J.; Linford, M. R.; Wigren, C.; Cao, R. Y.; Pianetta, P.; Chidsey, C. E. D., Determination of the bonding of alkyl monolayers to the Si(111) surface using chemical-shift, scanned-energy photoelectron diffraction. *Appl. Phys. Lett.* **1997**, 71, (8), 1056-1058.
29. Effenberger, F.; Gotz, G.; Bidlingmaier, B.; Wezstein, M., Photoactivated preparation and patterning of self-assembled monolayers with 1-alkenes and aldehydes on silicon hydride surfaces. *Angew. Chem., Int. Ed. Engl.* **1998**, 37, (18), 2462-2464.
30. Boukherroub, R.; Wayner, D. D. M., Controlled functionalization and multistep chemical manipulation of covalently modified Si(111) surfaces. *J. Am. Chem. Soc.* **1999**, 121, (49), 11513-11515.
31. Cicero, R. L.; Linford, M. R.; Chidsey, C. E. D., Photoreactivity of unsaturated compounds with hydrogen-terminated silicon(111). *Langmuir* **2000**, 16, (13), 5688-5695.
32. Buriak, J. M.; Allen, M. J., Lewis acid mediated functionalization of porous silicon with substituted alkenes and alkynes. *J. Am. Chem. Soc.* **1998**, 120, (6), 1339-1340.

33. Buriak, J. M.; Stewart, M. P.; Geders, T. W.; Allen, M. J.; Choi, H. C.; Smith, J.; Raftery, D.; Canham, L. T., Lewis acid mediated hydrosilylation on porous silicon surfaces. *J. Am. Chem. Soc.* **1999**, 121, (49), 11491-11502.
34. Mitchell, S. A.; Boukherroub, R.; Anderson, S., Second harmonic generation at chemically modified Si(111) surfaces. *J. Phys. Chem. B* **2000**, 104, (32), 7668-7676.
35. Yu, H. Z.; Boukherroub, R.; Morin, S.; Wayner, D. D. M., Facile interfacial electron transfer through n-alkyl monolayers formed on silicon (111) surfaces. *Electrochem. Commun.* **2000**, 2, (8), 562-566.
36. Bansal, A.; Li, X. L.; Lauermann, I.; Lewis, N. S.; Yi, S. I.; Weinberg, W. H., Alkylation of Si surfaces using a two-step halogenation Grignard route. *J. Am. Chem. Soc.* **1996**, 118, (30), 7225-7226.
37. Bansal, A.; Li, X. L.; Yi, S. I.; Weinberg, W. H.; Lewis, N. S., Spectroscopic studies of the modification of crystalline Si(111) surfaces with covalently-attached alkyl chains using a chlorination/alkylation method. *J. Phys. Chem. B* **2001**, 105, (42), 10266-10277.
38. Terry, J.; Linford, M. R.; Wigren, C.; Cao, R. Y.; Pianetta, P.; Chidsey, C. E. D., Alkyl-terminated Si(111) surfaces: A high-resolution, core level photoelectron spectroscopy study. *J. Appl. Phys.* **1999**, 85, (1), 213-221.
39. Okubo, T.; Tsuchiya, H.; Sadakata, M.; Yasuda, T.; Tanaka, K., An organic functional group introduced to Si(111) via silicon-carbon bond: A liquid-phase approach. *Appl. Surf. Sci.* **2001**, 171, (3-4), 252-256.
40. He, J.; Patitsas, S. N.; Preston, K. F.; Wolkow, R. A.; Wayner, D. D. M., Covalent bonding of thiophenes to Si(111) by a halogenation/thienylation route. *Chem. Phys. Lett.* **1998**, 286, (5-6), 508-514.
41. Allongue, P.; de Villeneuve, C. H.; Pinson, J.; Ozanam, F.; Chazalviel, J. N.; Wallart, X., Organic monolayers on Si(111) by electrochemical method. *Electrochim. Acta* **1998**, 43, (19-20), 2791-2798.
42. Strother, T.; Cai, W.; Zhao, X. S.; Hamers, R. J.; Smith, L. M., Synthesis and characterization of DNA-modified silicon (111) surfaces. *J. Am. Chem. Soc.* **2000**, 122, (6), 1205-1209.
43. Lin, Z.; Strother, T.; Cai, W.; Cao, X. P.; Smith, L. M.; Hamers, R. J., DNA attachment and hybridization at the silicon (100) surface. *Langmuir* **2002**, 18, (3), 788-796.
44. Pike, A. R.; Lie, L. H.; Eagling, R. A.; Ryder, L. C.; Patole, S. N.; Connolly, B. A.; Horrocks, B. R.; Houlton, A., DNA on silicon devices: On-chip synthesis, hybridization, and charge transfer. *Angew. Chem., Int. Ed.* **2002**, 41, (4), 615.
45. Yousaf, M. N.; Mrksich, M., Diels-Alder reaction for the selective immobilization of protein to electroactive self-assembled monolayers. *J. Am. Chem. Soc.* **1999**, 121, (17), 4286-4287.
46. Yeo, W. S.; Yousaf, M. N.; Mrksich, M., Dynamic interfaces between cells and surfaces: Electroactive substrates that sequentially release and attach cells. *J. Am. Chem. Soc.* **2003**, 125, (49), 14994-14995.
47. Kim, K.; Jang, M.; Yang, H. S.; Kim, E.; Kim, Y. T.; Kwak, J., Electrochemically induced and controlled one-step covalent coupling reaction on self-assembled monolayers. *Langmuir* **2004**, 20, (10), 3821-3823.

48. Pavlovic, E.; Quist, A. P.; Gelius, U.; Nyholm, L.; Oscarsson, S., Generation of thiolsulfonates/thiolsulfonates by electrooxidation of thiols on silicon surfaces for reversible immobilization of molecules. *Langmuir* **2003**, *19*, (10), 4217-4221.
49. Hong, H. G.; Park, W., Electrochemical characteristics of hydroquinone-terminated self-assembled monolayers on gold. *Langmuir* **2001**, *17*, (8), 2485-2492.
50. Giovanelli, D.; Lawrence, N. S.; Jiang, L.; Jones, T. G. J.; Compton, R. G., Electrochemical characterization of sulfide tagging via its reaction with benzoquinone derivatives. *Anal. Lett.* **2003**, *36*, (14), 2941-2959.
51. Roussel, C.; Rohner, T. C.; Jensen, H.; Girault, H. H., Mechanistic aspects of on-line electrochemical tagging of free L-cysteine residues during electrospray ionisation for mass spectrometry in protein analysis. *Chemphyschem* **2003**, *4*, (2), 200-206.
52. Zhu, X. Y.; Jun, Y.; Staarup, D. R.; Major, R. C.; Danielson, S.; Boiadjiev, V.; Gladfelter, W. L.; Bunker, B. C.; Guo, A., Grafting of high-density poly(ethylene glycol) monolayers on Si(111). *Langmuir* **2001**, *17*, (25), 7798-7803.
53. Clare, T. L.; Clare, B. H.; Nichols, B. M.; Abbott, N. L.; Hamers, R. J., Functional monolayers for improved resistance to protein adsorption: Oligo(ethylene glycol)-modified silicon and diamond surfaces. *Langmuir* **2005**, *21*, (14), 6344-6355.
54. Rohde, R. D.; Agnew, H. D.; Yeo, W. S.; Bailey, R. C.; Heath, J. R., A non-oxidative approach toward chemically and electrochemically functionalizing Si(111). *J. Am. Chem. Soc.* **2006**, *128*, (29), 9518-9525.
55. Dillmore, W. S.; Yousaf, M. N.; Mrksich, M., A photochemical method for patterning the immobilization of ligands and cells to self-assembled monolayers. *Langmuir* **2004**, *20*, (17), 7223-7231.
56. Kwon, Y.; Mrksich, M., Dependence of the rate of an interfacial Diels-Alder reaction on the steric environment of the immobilized dienophile: An example of enthalpy-entropy compensation. *J. Am. Chem. Soc.* **2002**, *124*, (5), 806-812.
57. Palegrosdemange, C.; Simon, E. S.; Prime, K. L.; Whitesides, G. M., Formation of self-assembled monolayers by chemisorption of derivatives of oligo(ethylene glycol) of structure HS(CH<sub>2</sub>)<sub>11</sub>(OCH<sub>2</sub>CH<sub>2</sub>)<sub>meta</sub>-OH on gold. *J. Am. Chem. Soc.* **1991**, *113*, (1), 12-20.
58. Haber, J. A.; Lewis, N. S., Infrared and X-ray photoelectron spectroscopic studies of the reactions of hydrogen-terminated crystalline Si(111) and Si(100) surfaces with Br-2, I-2, and ferrocenium in alcohol solvents. *J. Phys. Chem. B* **2002**, *106*, (14), 3639-3656.
59. Webb, L. J.; Lewis, N. S., Comparison of the electrical properties and chemical stability of crystalline silicon(111) surfaces alkylated using grignard reagents or olefins with Lewis acid catalysts. *J. Phys. Chem. B* **2003**, *107*, (23), 5404-5412.
60. Himpfel, F. J.; McFeely, F. R.; Talebibrabimi, A.; Yarmoff, J. A.; Hollinger, G., Microscopic structure of the SiO<sub>2</sub>/Si interface. *Phys. Rev. B* **1988**, *38*, (9), 6084-6096.
61. Higashi, G. S.; Chabal, Y. J.; Trucks, G. W.; Raghavachari, K., Ideal hydrogen termination of the Si-(111) surface. *Appl. Phys. Lett.* **1990**, *56*, (7), 656-658.
62. Hirose, M.; Yasaka, T.; Takakura, M.; Miyazaki, S., Initial oxidation of chemically cleaned silicon surfaces. *Solid State Technol.* **1991**, *34*, (12), 43-48.

63. Yasaka, T.; Takakura, M.; Sawara, K.; Uenaga, S.; Yasutake, H.; Miyazaki, S.; Hirose, M., Native oxide growth on hydrogen-terminated silicon surfaces. *IEICE Trans. Electron.* **1992**, E75C, (7), 764-769.
64. Miura, T.; Niwano, M.; Shoji, D.; Miyamoto, N., Kinetics of oxidation on hydrogen-terminated Si(100) and (111) surfaces stored in air. *J. Appl. Phys.* **1996**, 79, (8), 4373-4380.
65. Bansal, A.; Lewis, N. S., Stabilization of Si photoanodes in aqueous electrolytes through surface alkylation. *J. Phys. Chem. B* **1998**, 102, (21), 4058-4060.
66. Barrelet, C. J.; Robinson, D. B.; Cheng, J.; Hunt, T. P.; Quate, C. F.; Chidsey, C. E. D., Surface characterization and electrochemical properties of alkyl, fluorinated alkyl, and alkoxy monolayers on silicon. *Langmuir* **2001**, 17, (11), 3460-3465.
67. Prime, K. L.; Whitesides, G. M., Adsorption of proteins onto surfaces containing end-attached oligo(ethylene oxide) - a model system using self-assembled monolayers. *J. Am. Chem. Soc.* **1993**, 115, (23), 10714-10721.
68. Stromme, M.; Niklasson, G. A.; Granqvist, C. G., Determination of fractal dimension by cyclic I-V studies: The Laplace-transform method. *Phys. Rev. B* **1995**, 52, (19), 14192.
69. Rohner, T. C.; Rossier, J. S.; Girault, H. H., On-line electrochemical tagging of cysteines in proteins during nanospray. *Electrochem. Commun.* **2002**, 4, (9), 695-700.
70. White, P. C.; Lawrence, N. S.; Davis, J.; Compton, R. G., Electrochemically initiated 1,4 additions: a versatile route to the determination of thiols. *Anal. Chim. Acta* **2001**, 447, (1-2), 1-10.
71. Newman, G. R.; Jasani, B., Silver development in microscopy and bioanalysis: Past and present. *J. Pathol.* **1998**, 186, (2), 119-125.
72. Bunimovich, Y. L.; Shin, Y. S.; Yeo, W. S.; Amori, M.; Kwong, G.; Heath, J. R., quantitative real-time measurements of DNA hybridization with alkylated nonoxidized silicon nanowires in electrolyte solution. *J. Am. Chem. Soc.* **2006**, 128, (50), 16323-16331.
73. Hansen, K. M.; Ji, H. F.; Wu, G. H.; Datar, R.; Cote, R.; Majumdar, A.; Thundat, T., Cantilever-based optical deflection assay for discrimination of DNA single-nucleotide mismatches. *Anal. Chem.* **2001**, 73, (7), 1567-1571.
74. McKendry, R.; Zhang, J. Y.; Arntz, Y.; Strunz, T.; Hegner, M.; Lang, H. P.; Baller, M. K.; Certa, U.; Meyer, E.; Guntherodt, H. J.; Gerber, C., Multiple label-free biodetection and quantitative DNA-binding assays on a nanomechanical cantilever array. *Proc. Natl. Acad. Sci., U.S.A.* **2002**, 99, (15), 9783-9788.
75. Kim, K.; Hwang, J.; Seo, I.; Youn, T. H.; Kwak, J., Protein micropatterning based on electrochemically switched immobilization of bioligand on electropolymerized film of a dually electroactive monomer. *Chem. Commun.* **2006**, (45), 4723-4725.
76. Stern, E.; Jay, S.; Bertram, J.; Boese, B.; Kretzschmar, I.; Turner-Evans, D.; Dietz, C.; Lavan, D. A.; Malinski, T.; Fahmy, T.; Reed, M. A., Electropolymerization on microelectrodes: Functionalization technique for selective protein and DNA conjugation. *Anal. Chem.* **2006**, 78, (18), 6340-6346.
77. Choi, I. S.; Chi, Y. S., Surface reactions on demand: Electrochemical control of SAM-based reactions. *Angew. Chem., Int. Ed.* **2006**, 45, (30), 4894-4897.

78. Devaraj, N. K.; Dinolfo, P. H.; Chidsey, C. E. D.; Collman, J. P., Selective functionalization of independently addressed microelectrodes by electrochemical activation and deactivation of a coupling catalyst. *J. Am. Chem. Soc.* **2006**, 128, (6), 1794-1795.
79. Streifer, J. A.; Kim, H.; Nichols, B. M.; Hamers, R. J., Covalent functionalization and biomolecular recognition properties of DNA-modified silicon nanowires. *Nanotechnology* **2005**, 16, (9), 1868-1873.
80. Curreli, M.; Li, C.; Sun, Y. H.; Lei, B.; Gundersen, M. A.; Thompson, M. E.; Zhou, C. W., Selective functionalization of In<sub>2</sub>O<sub>3</sub> nanowire mat devices for biosensing applications. *J. Am. Chem. Soc.* **2005**, 127, (19), 6922-6923.
81. Bunimovich, Y. L.; Ge, G.; Beverly, K. C.; Ries, R. S.; Hood, L.; Heath, J. R., Electrochemically programmed, spatially selective biofunctionalization of silicon wires. *Langmuir* **2004**, 20, (24), 10630-10638.